Application of a Novel AAV Gene Therapy: Investigating AAV6.2-FF in Models of Pulmonary Surfactant-Related Disease

Kennedy Nangle

A thesis submitted to the University of Ottawa in partial fulfillment of the requirements for the Master's degree in Cellular and Molecular Medicine specialized in Human and Molecular Genetics

Department of Cellular and Molecular Medicine, School of Graduate Studies
Faculty of Medicine
University of Ottawa

ABSTRACT

Surfactant proteins are a group of proteins responsible for maintaining a healthy lung by lowering surface tension in the alveoli and facilitating proper homeostasis of pulmonary surfactant components at the air-liquid interface. Surfactant protein B and C have been associated with disease as a result of genetic mutations disrupting the function of these critical proteins. Mutations in the Surfactant protein C gene (*SFTPC*) are known to cause Pulmonary Fibrosis (PF), a rare, chronic, lethal lung condition characterized by the build up of scar tissue in the pulmonary space. Mutations in the *SFTPB* gene are associated with a rare, lethal condition, SP-B deficiency. This condition presents neonatally and is characterized by respiratory distress and neonatal death within the first weeks of life. There are currently no treatments for either condition and lung transplantation is the only opportunity for a cure. The clear genetic etiology of both conditions offers the possibility of treatment through gene therapy.

Recently, our lab has shown the potential of a novel viral vector gene therapy (AAV6.2-FF) for the treatment of SP-B deficiency, restoring expression of the *Sftpb* gene and extending the lifespan of SP-B deficient mice by over 300+ days compared to controls. Additionally, our lab has extended the use of this gene therapy platform for the treatment for *Sftpc*-related pulmonary fibrosis in a transgenic mouse model of the most common mutation (I73T) associated with the disease (manuscript in review). This thesis focuses on a potential therapy transfer of the *Sftpc* gene therapy to another common *SFTPC* mutation, L184Q. This thesis also addresses the characterization of re-administration of the AAV6.2-FF vector in *Sftpb* mice in order to expand on the potential clinical translation of the therapy. Both models were established and feasibility of the therapeutic expansion of these models was assessed. In the model of *Sftpc*-L184Q knock-in, the administration of bleomycin resulted in a significant increase in fibrosis, as measured by the Ashcroft-Hubner score, a significant change in lung structure, by proxy of the Mean Linear Intercept, and a significant decrease in lung function. Taken together, this demonstrates the successful development of injury in this mouse model. The administration of the AAV6.2-FF gene therapy resulted in a significant expression of the *Sftpc* transgene in the lung tissue of the L184Q mice, demonstrating the potential of the therapeutic in the L184Q model. Further studies assessing the combination of the injury model and administration of the therapeutic are required. A difference in phenotype between LQ and I73T mice was explored and investigations into this phenotype have laid the foundation for future exploration.

ABBREVIATIONS

ATII	Alveolar Type II
AH	Ashcroft-Hubner score
BLM	Bleomycin
chILD	Childhood Interstitial Lung Disease
COPD	Chronic Obstructive Pulmonary Disease
Ds-DNA	Double-stranded DNA
ECM	Extracellular Matrix
ER	Endoplasmic Reticulum
FOV	Field of View
IIP	Idiopathic Interstitial Pneumonia
ILD	Interstitial Lung Disease
IP	Intraperitoneal
IPF	Idiopathic Pulmonary Fibrosis
IT	Intratracheal
IIP	Idiopathic Interstitial Pneumonia
KI	Knock-in
KO	Knock-out
LB	Lamellar Body
LQ	L184Q
mature SP-C	Mature Surfactant Protein C
MLI	Mean Linear Intercept
OS	Oxidative Stress
PIP	Peak Inspiratory Pressure

PV	Pressure-volume
RDS	Respiratory Distress Syndrome
RLW	Right Lung Weight
ROS	Reactive Oxygen Species
SALI	Surfactant-Air-Liquid Interface
SP-A/B/C/D	Surfactant protein A/B/C/D
UPR	Unfolded Protein Response
WT	Wildtype

TABLE OF CONTENTS

LIST OF TABLES

LIST OF FIGURES

ACKNOWLEDGEMENTS

There are many people who have contributed to this thesis in ways that reach from academic and scientific contributions to support throughout the process. I feel beyond grateful to have the opinions and expertise of each individual throughout the process.

Thank you to all academic contributors and collaborators that helped make this project possible. To my Thesis Advisory Committee, thank you for your valuable input that shaped the progression of this project throughout the 2 years. Thank you to our collaborators at the Wootton Lab (University of Guelph) for producing the AAV product that without which, this project would not be made possible. Thank you to the ACVS Staff and the Histology Core at the University of Ottawa for your care, hard work and expertise with all samples.

A sincere and profound thank you to my colleagues in the Xplore Laboratory who have all been such willing and patient teachers. Thank you to Li for your contributions, since training me in the beginning. It was such a pleasure to learn from you. Arul and Shumei, you are so central to all the work that is done at the Lab, and I thank you for your work at every harvest. Ewa, your generosity of spirit and curiosity fuelled an exciting lab dynamic. Your empathy and guidance in both personal and professional situations is something I aspire to. Adi and Mahnaz, thank you for your support. Your camaraderie as fellow colleagues is appreciated. Dr. Chanele Cyr-Depauw, Dr. Wojtek Durlak and Dr. Martin Kang, I am so appreciative of your expertise and thoughtful input over the last 2 years. Thank you to each and every person at the XPlore Lab with whom this work would not have been made possible. I have not only learned from each of you but have also forged friendships.

Dr. Thebaud, my supervisor, I would like to thank you for the vision, drive, and hope that you bring to the lab. Your lens is meaningful to a young student, bringing a human perspective to the often non-human work we do. Thank you also for your patience and understanding as I navigated both the scientific and professional realms for the first time.

My greatest and deepest gratitude is owed to Dr. Pauline Bardin. Pauline, you have been a scientific mentor, a personal mentor, and a friend to me over the past years. Learning from you in the lab made me find a stronger voice, and recognize my value. Being your student in this work was a privilege. Thank you for your compassion and your friendship.

On a personal note, thank you to my partner, my family and my friends for your unconditional support. Thank you to my parents for an unforgettable two years. Jack, I could not do this without you. Maya, my best friend, your support means the world.

My deepest gratitude to each individual who has helped or contributed to this work in some way, whether through support or scientific input - I am unbelievably appreciative

1. INTRODUCTION

1.1 Pulmonary surfactant

1.1.1 Function and physiology of pulmonary surfactant

The lung is composed of a complex organization of epithelial surfaces that maximize area for gas exchange and facilitate proper breathing. The terminal and smallest structure of the lung, the alveolus, is a bulb-like structure that facilitates gas exchange of oxygen from air into the bloodstream, allowing oxygenation of proximal and distal tissues[1]. The lung is one of a few surfaces in direct contact with the external environment and there are many biological defences to ensure this organ remains in a healthy state. As such, the alveoli of the lung are lined with a liquid phase, composed primarily of water to prevent desiccation[2]. Water lining a space such as the alveoli presents an additional issue, as intermolecular forces between water molecules are high. Without the interruption or distribution of these intermolecular forces, high surface tension in the alveoli render these structures susceptible to collapse, clinically titled atelectasis. In order to prevent atelectasis, epithelial cells of the lung or alveolar type II (ATII) cells produce a substance called pulmonary surfactant, which is required for maintaining a low surface tension in the alveoli[2].

Pulmonary surfactant is produced and secreted only by ATII cells. The components of pulmonary surfactant are responsible for maintaining a low surface tension and a protective barrier to the external environment as a result of their molecular properties[2,3]. Surfactant is composed of lipids, proteins, and organic molecules. About 90% of pulmonary surfactant is composed of phospholipids, the most common of which is phosphatidylcholine[4]. The hydrophobic phospholipids of pulmonary surfactant line the water phase of the airway in order to disrupt the high surface tension present between water molecules in this small space. There are four surfactant proteins (A, B, C, and D) present in pulmonary surfactant, each possessing

varying molecular properties that enable their specific function[4]. The components of pulmonary surfactant, including some proteins and phospholipids, are secreted into the airway through a cell-type specific organization of intracellular surfactant, the Lamellar Body (LB)[5]. Lamellar bodies are responsible for the secretion of critical components of surfactant and are made up of multiple, concentric layers of phospholipid membranes. Surfactant proteins B and C are integrated into these concentric membranes and are secreted into the air space, where the LB unwinds to expose its components and interacting with the environment of the alveolar lumen. Here, surfactant proteins carry out their essential functions[5].

1.1.2 The Role of Surfactant Proteins

Specifically, Surfactant protein A and surfactant protein D are both responsible for surfactant homeostasis and immunity at the air-lung surface. Surfactant protein A (SP-A) is a 26-35kDa lipid-associated protein and it's various isoforms are present in surfactant, leading to the wide variety of functions associated with the protein[6]. Studies have shown that SP-A facilitates tubular myelin formation and enhances the biophysical activity of pulmonary surfactant. Importantly, SP-A has also been demonstrated to have an important function in the innate immune defence of the lung by enhancing binding, uptake and phagocytosis of various pathogens. Surfactant protein D (SP-D) is 43 kDa in size, and unlike other surfactant proteins, it is expressed throughout the body in organs such as the bile duct and the gastro-intestinal tract. In the lung, SP-D is highly expressed by ATII cells and is also expressed by other airway epithelial cells[6,7,8]. Both *in vitro* and *in vivo* studies have shown that SP-D is important in the innate immune response as it's globular carbohydrate recognition domain has a high binding affinity for bacterial lipopolysaccharides and other carbohydrates found on the surface of various bacteria, fungi, and viral pathogens. SP-D has been shown to agglutinate these pathogens, increasing their

uptake by resident alveolar macrophages. It is also hypothesized that SP-D may influence the acquired immune response, in addition to the innate response[8]. SP-D has also demonstrated a role in surfactant homeostasis as *Sftpd* deletion in transgenic mice resulted in pulmonary lipidosis and an increase in the surfactant lipid pool size[9]. Both SP-A and SP-D play a role in the maintenance of a healthy pulmonary environment through both surfactant lipid regulation and innate immune response.

Surfactant proteins B and C function to maintain a low alveolar surface tension and proper surfactant metabolism. The active form of surfactant protein B (SP-B) is a small hydrophobic protein composed of 79 amino acids, encoded by the *SFTPB* gene, located on chromosome 2p11.2. SP-B is expressed minimally in most airway cells but is highly expressed in ATII cells where it undergoes extensive proteolytic processing to reach it's active form[11]. In the active form, SP-B is transferred from multi-vesicular bodies to LBs, where it is secreted into the alveolar lumen. SP-B is known to function in the formation of LBs, lipid layers at the air phase of the alveolar lumen, and distribution phospholipids throughout surfactant, all of which contribute to preventing atelectasis[12,13]. *In vivo,* deletion of *SFTPB* results in the rapid development of respiratory distress, atelectasis, and death in mice at birth, demonstrating the critical role of this protein in respiration. Overall, SP-B is responsible for enhancing stability of the alveoli and spreading of surfactant[12].

While various functions of Surfactant protein C (SP-C) and SP-B are known to overlap, unlike SP-B, SP-C is not necessary for proper respiration and lung function. SP-C is encoded by the *SFTPC* gene located on chromosome 8p21.3[11,12]. The *SFTPC* gene is highly conserved and highly tissue specific, as it is only transcribed in ATII cells. The transcription and translation of the *SFTPC* gene results in a 197-amino acid pro-peptide (proSP-C) containing an N-terminal

domain and a C-terminal BRICHOS domain[14]. The proSP-C N-terminal domain is known to direct trafficking of the peptide throughout the cell for cleavage while the BRICHOS domain of the SP-C protein facilitates proper folding of the transmembrane protein domain[15]. Both are ultimately cleaved following proper intracellular trafficking and transmembrane insertion. The pro-peptide undergoes extensive processing and folding throughout the cell to reach it's mature form (matureSP-C or mSP-C). The proSP-C peptide is trafficked throughout the alveolar cell from the Golgi apparatus to the apical surface of the ATII cells. From the apical membrane, proSP-C undergoes endocytosis and is then trafficked to multi-vesicular bodies for further cleavage[15]. From the multi-vesicular body, SP-C is trafficked to ATII cell-specific lamellar bodies for final processing and secretion of mSP-C. The mature form of SP-C is a small, 4.2kDa protein which is highly hydrophobic and consists of 35 amino acids (Figure 1).

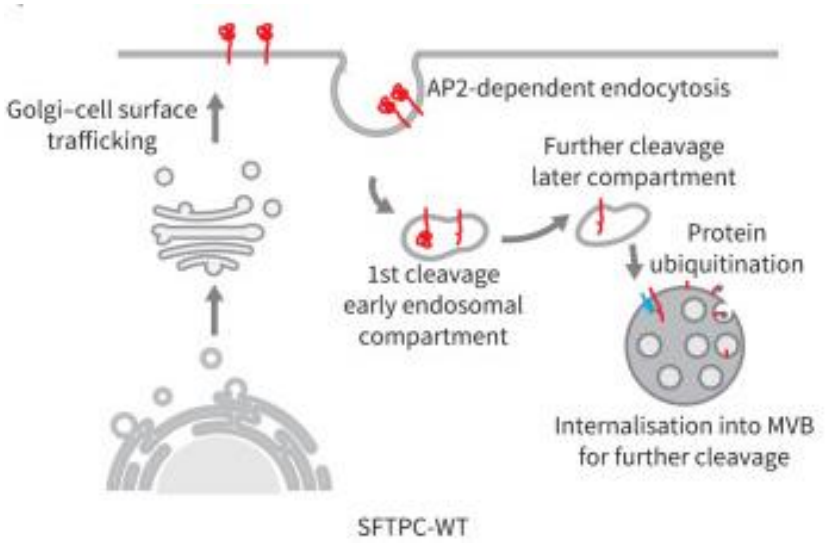

Figure 1. Trafficking and processing of the proSP-C peptide into the mature SP-C peptide (Dickens et al. 2022)

SP-C is the most abundant surfactant protein in the lung by molar weight and is a transmembrane protein which exists in semi-stable alpha-helices. SP-C has many functions in both ATII cells and at the air-liquid interface in pulmonary surfactant. It is primarily responsible for reducing surface tension in the terminal lung and helping prevent alveolar collapse. As a result of the transmembrane localization and the highly hydrophobic nature of mSP-C, it is known to distribute lipids throughout pulmonary surfactant film and facilitate homeostasis of surfactant composition[15]. As a highly hydrophobic protein, SP-C functions to spread lipids into a monolayer at the air-liquid interface, repelling the highly abundant phospholipids, facilitating lipid motion and distribution. Additionally, the hydrophobic nature of the protein has been shown to help capture and re-spread surfactant lipids across the alveolar surface upon exiting the alveoli during compression of the lung at exhalation. This function is considered highly important as surfactant lipid formation and distribution throughout the terminal lung is responsible for maintaining a low surface tension and thus preventing alveolar collapse at end-expiration[15].

This healthy expression and highly organized secretion of the mature SP-C protein therefore aids in a healthy biophysical function of the alveoli. The dynamic and multi-functional nature of this protein makes it a highly important molecule in regulating the surface of the alveoli and the air-liquid interface. Together, surfactant proteins maintain a functional pulmonary barrier, carrying out critical biophysical and immune functions while promoting proper respiration.

1.2 Surfactant Proteins in Disease

Surfactant proteins contribute to healthy respiration through their metabolic and immune properties as previously established. Issues in surfactant protein regulation, development, and production are known to be associated with pulmonary disease. Altered or aberrant expression of surfactant proteins has been linked to pulmonary disease of both genetic and multifactorial

etiologies. In fact, pathogenic mutations in surfactant protein genes *SFTPB, SFTPC,* and *ABCA3* are all well-characterized causes of of neonatal respiratory distress syndrome (RDS), childhood interstitial lung disease (chILD), and pulmonary fibrosis[12]. Ultimately with deficient surfactant protein B and C, respiration is impacts as a result of altered surface tension in the alveoli (Figure 2).

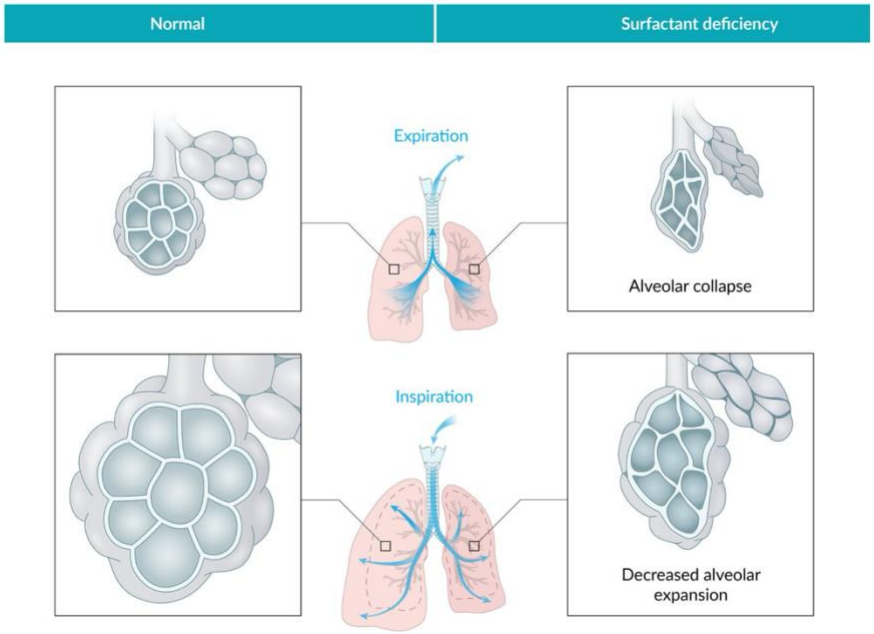

Figure 2. Effects of surfactant deficiency on respiration. Image retrieved from AMBOSS (Amboss. (n.d.). https://www.amboss.com/us/knowledge/neonatal-respiratory-distress-syndrome).

1.2.1 Genetic causes of Surfactant Protein-Related Disease

1.2.1.1 Surfactant Protein B Deficiency

Surfactant protein B (SP-B) deficiency is a rare, autosomal recessive condition caused by mutations in the *SFTPB* gene, leading to a significant reduction in the amount SP-B protein by non-sense mediated decay of the mRNA transcript. SP-B deficiency has an estimated incidence of 1 in 1.5 million births and is also estimated to account for 10% of unexplained respiratory failure in infants[5]. The most common pathogenic variant causing SP-B deficiency is

Pro133Glnfs*95, an insertion causing a frameshift and thus, an altered mRNA transcript which is targeted for mRNA-mediated decay. SP-B deficiency presents neonatally and is characterized by neonatal RDS and progressive respiratory failure. This lethal condition usually results in death before 2 months of age[16]. The critical role of SP-B in respiration is thus highlighted by the clinical context of SP-B deficiency. The SP-B protein is required for respiration, as it is responsible for surfactant phospholipid homeostasis through the biosynthesis of lamellar bodies in ATII cells and the organization of tubular myelin in surfactant. It ultimately allows for the spreading of intermolecular forces in the alveoli and prevents alveolar collapse. Neonates therefore undergo alveolar collapse and increased surface tension of the alveoli when biallelic pathogenic variants of *SFTPB* produce insufficient levels of healthy SP-B protein[11]. Attempts to treat SP-B deficiency typically involve treatment with exogenous, SP-B-enriched surfactant. However, surfactant replacement is a short-term therapeutic treatment as surfactant is metabolized quickly in the lung and must be re-administered frequently. The only known cure for SP-B deficiency is lung transplantation. However, this treatment is exceedingly rare and presents a multitude of challenges with a lack of donors, growth, and suitability of lungs during the neonatal period. SP-B deficiency is a clear example of the pathogenesis which occurs with surfactant protein dysfunction.

1.2.1.2 Surfactant Protein C Related Pulmonary Fibrosis

Mono-allelic mutations in the *SFTPC* gene, encoding the SP-C protein, have also been associated with autosomal disease, specifically pulmonary fibrosis, inflammation, interstitial lung disease (ILD) and less commonly, neonatal RDS[11,15]. The prevalence of *SFTPC*-related disease is not currently known. Childhood and infantile onset of these pulmonary conditions have been observed in infants, as well as adult-onset pulmonary fibrosis and interstitial lung

disease, demonstrating the variable penetrance of *SFTPC* pathogenic variants. There is a wide range in both the disease and the age of onset of these conditions due to pathogenic *SFTPC* mutations. Mutations in *SFTPC* are known to arise *de novo* or can be inherited through families. The most common *SFTPC* mutation is p.Ile73Thr (I73T), which accounts for about 30-40% of all cases of pulmonary disease induced by *SFTPC* mutations, and is located outside the BRICHOS domain[15,21]. I73T has been associated with cases of childhood interstitial lung disease (chILD) specifically, reported in both sporadic and inherited cases. The I73T mutation causes aberrant trafficking of proSP-C leading to accumulation of proSP-C to toxic levels in ATII cells as the protein is not properly trafficked to lamellar bodies. The abnormally processed pro-peptide accumulates and blocks autophagy which triggers apoptosis of the cell. ATII are considered progenitor cells of the lung as they maintain the lung cell population and give rise to ATI cells[15]. Both widespread apoptosis resulting in depletion of the lung cell population and, protein aggregation is thought to lead to pulmonary fibrosis and chILD as a result of the I73T mutation. Mutations in the BRICHOS domain of the SP-C protein have also been found in familial cases of lung disease including pneumonitis in children and interstitial lung disease in adults which is the histological correlate to idiopathic pulmonary fibrosis (IPF)[21]. The L188Q mutation was identified in a large family of over 300 individuals, resulting in many individuals experiencing variable lung disease in a dominant mode of inheritance with variable penetrance and expressivity[22]. The location of this mutation in the BRICHOS domain leads to an improperly folded proSP-C protein. The improper folding of the proSP-C protein leads to it's retention within the endoplasmic reticulum and the accumulation of a toxic pro-protein in the form of cytosolic aggregates[21]. This ultimately actives the unfolded protein response (UPR) and leads to endoplasmic reticulum (ER) stress[23,24]. ER stress was identified in patients with the L188Q

mutation. This cascade of events following ER stress has also been found to cause inflammatory signalling in ATII cells. The prolonged activation of ER stress has importantly been known to trigger apoptosis and contribute to lung injury[21,23,24].

1.2.1.3 Modelling Surfactant Protein Disorders

The need for preclinical models of ATII cell disorders is crucial to the development of therapeutics and understanding of disease. These preclinical models must also properly recapitulate the mainstays of the human condition in order to act as proper proxy for eventual therapeutic translation. Over time, the modelling of ATII cell-specific conditions has proven to be challenging due to the main features of this cell population and difficulties imitating the physiological lung environment.

1.2.1.3.1 In vitro Models of Surfactant Protein Disorders

In vitro modelling of ATII cells has been shown to be quite complex, involving complicated and time-consuming procedures which require special equipment and media. ATII cells are a progenitor cell population of the lung, giving rise to ATI cells[25]. In culture, ATII cells tend not to maintain their phenotype and differentiate into alveolar type I epithelial cells and contributes to a low yield of cells from culture, despite a long and complex procedure. Maintaining an ATII cell phenotype and halting the progression of daughter cells to ATI cells has been described as a significant challenge with ATII cell cultures. In order to overcome these challenges, *in vitro* models have evolved to include mechanisms which block progenitor activity. One study found that introducing an exogenous agent, interleukin-13, in culture blocks progenitor cell activity[26]. In fact, IL-13 was found to disrupt normal ATII cell differentiation *in vitro* by promoting a hyperplastic ATII cell phenotype which is commonly found in IPF patients[26]. These results align with clinical findings, as variants in *IL-13* have been associated

with worse pulmonary function in patients with IPF and this cytokine has been found to be up-regulated in bronchoalveolar lavage fluid of IPF patients. IL-13 is known to cause fibroblast activation through the TGF-ß pathway, along with many other cytokines, highlighting their contribution to an IPF phenotype while simultaneously disrupting the self-renewal of ATII cells and therefore growth and differentiation of the terminal lung. Blocking the differentiation of ATII cells to ATI cells therefore increases the yield of this culture for *in vitro* studies and has led to significant improvements in the study of the alveolar epithelium in culture[26]. Although these developments have been important in understanding the nature of ATII cells, typical ATII cell culture still does not properly capture the complex structure and physiological environment required for the study of surfactant proteins, as both the structure of the alveoli and the exposure to air is essential for surfactant production. Organoid cultures of the alveolar epithelium, called alveolarspheres, have also been a promising area of *in vitro* modelling as they better capture the complex nature of the *in vivo* lung by facilitating cell-cell interaction and the interplay between ATII and ATI cells[25]. However, these organoid cultures require the presence of support cells and therefore introduce a challenging confounding factor and do not mimic the alveolar structure. Over time, culture methods have also evolved to recreate the air-liquid interface *in vitro* in order to study surfactant protein production and metabolism, a feature unique to this cell population. Surfactant air-liquid interface (SALI) cultures have been successful in studying surfactant proteins and associated disorders[28,29]. This is done by suspending ATII cell cultures and exposing them to air at the apical side using air-lift culture. The formation of a functional barrier has enabled modelling of functional pulmonary features of the functional air-liquid interface such as lamellar body production and surfactant protein production. Unlike organoid cultures, the administration of vector-based gene therapies in SALI cultures is successful and expands the

possibility of studying surfactant protein disorders by the CRISPR-Cas9 addition of pathogenic variants of surfactant protein genes[28]. This is an advantage of SALI culture as isolation and culture of patient samples with surfactant protein disorder is rare and presents significant challenges. In a SALI model, Munis et al were able to use this strategy to successfully knock-out *SFTPB* in culture and found that permeability was disrupted by complete lack of SP-B expression, demonstrating the disruption of the air-liquid interface similar to SP-B deficiency in humans[28].

The technical expansion of ATII cell culture has led to important milestones in the understanding of signalling pathways for ATII cell growth and differentiation and has enabled our understanding of disease process. While lung epithelium can be modelled *in vitro*, there are still gaps in recapitulating the functional component of the lung. The complex environment of the lung, including immune regulation and response to mechanical stimuli is difficult to model *in vitro*. Altogether, the limitations of *in vitro* models of surfactant protein disorders result in overall less biologically relevant studies.

1.2.1.3.2 In vivo Modelling of Surfactant Protein Disorders

In vivo models of surfactant protein disorders offer more suitable, biologically relevant studies of these conditions as the structure and complexity of the air-liquid interface is maintained. However, timing and management is a significant challenge in *in vivo* modelling for both of SP-C-related PF and SP-B deficiency.

In vivo models of SP-B deficiency have presented significant challenges, as complete lack of SP-B leads to respiratory distress, respiratory failure, and death within days in animal models. While this mimics the clinical situation, it drastically limits the study of treatment and disease characterization[29,30]. In order to model SP-B deficiency and the impacts on the lung

beyond genetic knock outs, models of surfactant depletion have previously been employed, but do not properly mimic the neonatal onset and severity of disease, as surfactant regenerates. Another promising strategy of modelling SP-B deficiency *in vivo* is induced knock-out of *Sftpb* using inducing factors such as doxycycline[29]. Inducible models allow for the controlled knock out and timing of therapeutic administration. In 2020, our lab published investigations of a novel viral vector, AAV6.2-FF, for the delivery of an *Sftpb* transgene in a mouse model of doxycycline-induced *Sftpb* knock-out[29]. The AAV6.2-FF vector is a specialized AAV vector developed by the Wootton Lab at the University of Guelph which has demonstrated significant potential for lung-specific treatments. The AAV6 serotype used as a base for this gene therapy platform has previously shown to be expressed at high levels in the lung epithelium. The AAV6.2-FF was also developed with specific changes to the capsid which facilitate heparin (AAV6.2) binding and evade ubiquitin-mediated degradation (Y445F and Y731F; AAV6.2-FF). All of these features contribute to this vector's ability to mediate expression in the lung[29]. In the model of SP-B deficiency, this specialized vector was used to deliver a copy of the wildtype murine copy of the *Sftpb* gene in order to restore expression. The delivery of the AAV6.2-FF-*Sftpb* to knock out mice extended their lifespan by over 300+ days compared to controls, which live on average 3-7 days following *Sftpb* knock-out[29]. The expression and successful delivery of the AAV6.2-FF vector was tracked using a Luciferase reporter transgene *in vivo*. Using IVIS imaging of the Luciferase reporter, the AAV6.2-FF vector mediated *Sftpb* transgene expression in the lung for over 200 days following a single administration[29]. Based on this study, the AAV6.2-FF vector system was identified to have significant potential for the delivery of a gene therapy product to the mouse lung to restore expression. Despite the promise of the aforementioned model, there are limitations surrounding the clinical relevance, due to the timing of the inducible knock out.

Clinically, lack of SP-B occurs immediately following birth and respiratory distress soon follows, however the timing of induced knock out does not occur until later in the life cycle of the mouse.

In vivo models of *SFTPC* changes are well-established, primarily with the use of transgenic mice to model known, causative genetic mutations. One model of *Sftpc*-related ILD used transgenic expression of the L188Q [L184Q in LQ mice] characterized the L184Q phenotype at early timepoints in the life of the mice, ranging from Postnatal day (P) 4 and 21[21]. This study found that the mutant proSP-C protein generated throughout the alveolarization process early in life led to high levels of oxidative stress (OS), and apoptosis[21]. The overall response generated by the toxic proSP-C product was shown to impact the regeneration capacity of the lung due to death of ATII cells and initiate multiple stress pathways in the lung. Importantly, the characterization of this model also found that, like many other transgenic models of pulmonary fibrosis, mice with mutations such as L184Q do not spontaneously experience pulmonary fibrosis[21]. Conditions such as ILD are often the result of accumulation of negative physiological effects over time and are progressive. Mice and other rodents have a limited lifespan which may limit their capacity to experience the accumulation of pulmonary effects over time. For this reason, bleomycin is typically used in models of pulmonary fibrosis in rodents. Only one model to date has demonstrated the capacity for spontaneous fibrosis in a mouse model of pulmonary fibrosis. This model used a knock-in model of I73T expression, the most common mutation found in *SFTPC* pulmonary fibrosis in humans. This inducible model used Tamoxifen to initiate the expression of the *Sftpc*-I73T mutation in a line of transgenic mice to find that upon expression of the I73T mutation, alveolitis and a fibrotic phenotype was demonstrated in the lung[31].

1.3 Pulmonary Fibrosis and Interstitial Lung Disease

1.3.1Pathogenesis and Clinical Context of IPF

As previously mentioned, genetic surfactant dysfunction is known to cause various forms of lung disease ranging in age of onset, disease type, expressivity, and penetrance, which often fall under the term 'interstitial lung disease' or ILD[32]. ILD is a grouping of conditions which are widely characterized by pulmonary fibrosis of different etiologies. This heterogenous group of conditions is typically split into 5 categories: exposure-related, idiopathic interstitial pneumonia (IIP), connective tissue disease, sarcoidosis, and other. These conditions are diagnosed based on histological, radiological, clinical criteria describing the nature of pulmonary fibrosis[33,34]. The many ILDs have over 100 known causes, including genetic disorder. Under the category of IIP, IPF is the most common disease, characterized by the combination between chronic inflammation of pulmonary tissue and uncontrolled scarring (fibrosis) of the lung tissue[34].

The pathophysiology of pulmonary fibrosis is the result of 3 main physiological events which occur in the lung, and thus the continuous cycle of fibrosis is initiated. Firstly, ATII cell dysfunction occurs as a result of recurrent injury to the cell[35]. The nature of the injury can vary. For example, intracellular accumulation of a toxic misfolded protein, as in the case with surfactant proteins can cause ATII cell injury. Environmental injury to ATII cells is also a common cause of pulmonary fibrosis, as seen with exposure to airborne toxins such as Asbestos or smoking, which are widely known to cause lung tissue injury[35]. Upon recurrent injury of ATII cells, and thus the release of cytokines, recruitment of immune cells, and repair-inducing factors such FGF and VEGF begin the activation of resident fibroblasts and recruitment of fibroblasts to the lung to repair said injury. Activated fibroblasts in the lung transition and mature into myofibroblasts which accumulate and begin secreting extracellular matrix (ECM). The secretion

and deposition of ECM stiffens and creates scar tissue, leading to issues with lung compliance and gas exchange. This continuous cycle thus leads to the progression of pulmonary fibrosis.

Together, these hallmarks result in a thickened, inflamed lung epithelium. Histologically, IPF is described as the destruction of the alveolar-capillary interface resulting from myofibroblast invasion into lung parenchyma[35]. The loss of alveolar structure leads to significantly reduced gas exchange efficiency in the distal lung. The thickened and inflamed lung tissue presents clinically as impaired gas exchange with dyspnea, fatigue with daily activity, and potential respiratory failure. There are many known causes of IPF or pulmonary fibrosis (PF), including infection, severe exposure to toxins, and genetic mutations[36]. IPF typically presents in adulthood, due to the nature of the condition, which relies on the accumulation of biological products like myofibroblasts and toxic protein[36]. While the condition typically presents later, the morbidity is reportedly high in IPF, with respiratory failure and death approximately 3-5 years following this diagnosis[37,38].

1.3.2 Pulmonary Fibrosis and Surfactant Protein Dysfunction

As discussed previously, PF is known to be inherited and caused by pathogenic variants in surfactant protein genes (e.g. *SFTPC, ABCA3*)[40,41]. The link between PF and *SFTPC* mutations, specifically 173T and L188Q, is clear in clinical reports which range in severity, age of onset, and clinical course, however establishing a strong pathogenic link between *SFTPC* variants and the development of PF[41]. Both the I73T linker domain mutation and the L188Q BRICHOS domain mutation are known to cause PF by mechanism of accumulation of the altered protein product leading to blocked autophagy and the accumulation of a toxic protein (proSP-C), respectively. In both cases, the aberrant pro-peptide causes apoptosis of ATII cells and triggers an inflammatory response in the lung. With this, the fibrosis pathway is initiated and the build up of

scar tissue in the lung occurs[42]. This established relationship between PF and *SFTPC* mutations is important as it offers the potential for a potential therapeutic target for further research.

1.4 Modelling Pulmonary Fibrosis

Pulmonary fibrosis is currently the main cause for lung transplantation and as previously established, further research surrounding accessible and low risk treatments are required. In recent years, there have been efforts to establish models of pulmonary fibrosis for this reasons, and many rodent models have successfully encapsulated the hallmarks of fibrosis and recapitulated fibrosis as best as possible. These models have been critical in better understanding the complexity of PF, and investigating potential treatments.

1.4.1 Bleomycin Induced Fibrosis

The most well-understood models of PF in rodents relies on bleomycin (BLM), a fibrosis-inducing agent which is considered the 'gold standard' for modelling fibrosis. Bleomycin was originally developed and used as a chemotherapeutic agent for cancer. However, many reports of patients experiencing pulmonary symptoms emerged following treatment. Bleomycin was initially thought to cause double -stranded DNA breaks (ds-DNA) in tumour cells, but adverse effects on other tissues such as the lung became apparent[43]. Indeed, BLM induces ds-DNA breaks and triggers the fibrotic pathway in lung tissue. BLM causes ds-DNA breaks in the presence of iron and oxygen and produces Reactive Oxygen Species (ROS), contributing inflammation and fibrosis of the lung[43]. The ROS production and DNA injury caused by BLM initiates the inflammatory response in the lung tissue, which then recruits immune cells to the tissue. Immune cells such as alveolar macrophages and lymphocytes produce cytokines and growth factors that signal both resident fibroblasts and fibroblasts from throughout the body to the lung. Upon recruitment, fibroblasts mature into myofibroblasts in the lung and

ultimately secrete extracellular matrix, which is also known as scar tissue, remodelling the affected tissue. The recruitment of fibroblasts by BLM is mediated by TGF-ß signalling initially triggered by pro-inflammatory cytokines such as IL-6 and 12[43].

The fibrotic property of BLM was quickly adapted for use in mammal models including mouse, rat, dog, rabbit, and primates[43]. Many models of BLM-fibrosis have now been established and range in route of administration, dosage, and number of administrations. The main advantage of the BLM-fibrosis model is the reproducibility and predictability of BLM *in vivo*. This agent is known to be very strong, and effects can typically be easily observed. BLM is predictable as it acts in a 28-day cycle *in vivo*[44,45]. Following administration, most commonly by intratracheal (IT) injection, BLM immediately induces apoptosis and inflammation. This initial phase lasts for approximately 7 days. The following 3 days can be described as a transition period from acute lung injury to the fibrotic stage, shifting from a highly inflammatory profile to a fibrosis phenotype. The fibrosis stage persists for approximately 28 days, when spontaneous resolution of fibrosis can be observed in rodent models[46]. The spontaneous resolution of fibrosis is the main limitation of the model, as it does not mimic the human condition, characterized by chronic inflammation and progressive scarring throughout the lifetime. Additionally, multiple administrations of BLM have been investigated and demonstrated that timed, recurrent administration of BLM can better model chronic fibrosis and produce a more persistent fibrosis in mice. While this is the main critique of models of fibrosis, it remains the gold-standard for modelling this condition[43]. Other models of fibrosis have also been developed using strategies such as silica/asbestos, irradiation, and fluorescence isothiocyanate[43]. However, these models have significant limitations in timing of development and reproducibility.

Preclinical animal models such as BLM-induced fibrosis are imperative to ensure proper understanding of disease pathogenesis and facilitate the safe and feasible development of therapeutics which can ultimately be used to treat human conditions.

1.5 Therapeutics for Surfactant Protein Disorders and Surfactant Protein-related PF

Many preclinical models of surfactant protein disorders such as SP-C-related PF and SP-B deficiency have been successfully used to establish therapeutics for these conditions. However, there are currently no cures for either PF of SP-B deficiency besides lung transplantation and, on it's own, IPF is the most common reason for lung transplantation in North America[29,47]. This demonstrates the need for further investigations into therapeutics for both conditions.

The two main medications used for IPF are Nintedanib and Pirfenidone. These are both anti-fibrotic drugs which target inflammation and the proliferation of fibroblasts in order to slow continuous accumulation of fibroblasts triggered by inflammation[50]. While these drugs are known to attenuate symptoms and improve quality of life, they do not significantly impact the lifespan of patients. There is thus a need for low risk, accessible therapeutics which in fact improve life expectancy following diagnosis.

1.5.1 Current and Future Treatment of Pulmonary Fibrosis

Prior to the current standard for treatment of IPF, antifibrotic drugs, there were no known specific treatments for the condition. Medical professionals historically used steroid medications such as prednisolone to reduce inflammation, the precursor to fibrosis. At the time, this practice had little clinical data to support it. When investigated, it was found that combination treatment with immune-modulatory and steroid medication for IPF led to higher rates of death[50]. This resulted in a drastic shift in the field and led to the development of novel antifibrotic drugs, pirfenidone and nintedanib, for the treatment of IPF. These drugs slow the progression of the

condition by mediating the immune response and limiting fibroblast proliferation. Pirfenidone is both an anti-inflammatory agent and is known to reduce the proliferation of fibroblasts in the lung. While the mechanism is not fully understood, Pirfenidone is known to act through the TGF-ß pathway which contributes to fibrosis. The ASCEND trial which led to the approval of pirfenidone by the FDA demonstrated the longterm safety and efficacy of the drug, reducing mortality in patients by 50% and significantly slowing disease progression[51,52].

Nintedanib is another commonly prescribed antifibrotic drug for IPF. Nintedanib acts through anti-fibrotic and anti-angiogenic mechanisms by suppressing the growth factor-releasing signalling pathway which induces the process of fibrosis. It is a tyrosine kinase inhibitor acting on FGF and PDGF receptors to block the activation of proliferative pathways and fibroblast migration. Nintedanib is also highly anti-inflammatory as it acts to suppress TGF-ß, which is known to be involved in the process of inflammation[48,49]. The first trial for Nintedanib found a reduction in time to first exacerbation and a reduction is progression following treatment[53]. In mice, Nintedanib has been shown to reduce bleomycin-induced fibrosis, inflammation, apoptosis, and oxidative stress (OS) reactions through the Akt/mTOR pathways[49].

Treatments are currently under investigation for a low-risk, non-invasive treatment for IPF which improves the lifespan of patients. As fibrosis is a dynamic and complex process, there are many possible therapeutic targets demonstrating promise in the pharmaceutical pipeline. The immune system is known to stimulate the migration and proliferation of fibroblasts in the lung, making immune system regulation a suitable therapeutic target for fibrosis. An example of this would be the Recombinant Pentraxin 2 (rhPTX-2, PRM-151)[38]. This recombinant protein was shown to reduce fibroblast differentiation and immune cell infiltration in the lung in a model of BLM-induced fibrosis. Treatment of IPF with rhPTX-2 is currently in Phase III of a clinical trial

to assess efficacy but has demonstrated a reduction in adverse events and a reduction in symptoms in Phase I & II[38]. Beyond the many possible molecular targets which may be suitable for the general IPF, potential therapeutic strategies for PF arising from genetic etiologies may differ.

1.5.2 Current and Future Treatment of Surfactant Protein Deficiencies

The current landscape of treatment for SP-B deficiency is limited. As mentioned, lung transplantation is the only known cure for this condition, but the procedure is rare and has a high rate of mortality. The neonatal onset of SP-B deficiency makes transplantation especially challenging as well-matched neonatal donors are difficult to find and, donated lungs must fit and grow along with the recipient[29]. With this, there are no known therapies available for those born with SP-B deficiency, aside from delivery of exogenous surfactant, a transient and short-term therapy which temporarily improves levels SP-B protein present in surfactant. There are research efforts in gene addition and editing therapies which demonstrate promise for the possibility of a minimally invasive treatment of this condition, including the AAV6.2-FF-*Sftpb* system explored by our lab which demonstrates significant promise for the future of treatment for this condition[29].

The current landscape for treatment of *SFTPC*-related pulmonary fibrosis is also limited with no current treatments or clinical trails targeting the genetic etiology of this condition. The current treatment involves the regular administration of antifibrotic drugs. The development of a genetic-based therapeutic which could be applied to the known *SFTPC* mutations may address a significant proportion of PF cases and offer patients a non-invasive, single administration treatment for the condition. Additionally, the development of a single treatment which could be applied to many mutations related to the same condition could offer a beneficial therapeutic strategy for pulmonary fibrosis.

2. RATIONALE AND APPROACH

2.1 Rationale

Surfactant proteins are a group of proteins responsible for maintaining a healthy lung by lowering surface tension in the alveoli and facilitating proper homeostasis of pulmonary surfactant components at the air-liquid interface. Surfactant protein B and C have been associated with disease as a result of genetic mutations disrupting the function of these critical proteins.

Mutations in the Surfactant protein C gene (*SFTPC*) are known to cause Pulmonary Fibrosis (PF). PF is a rare, chronic, lethal lung disease characterized by inflammation and progressive build up of scar tissue in the interstitial space of the lungs. This ultimately leads to issues with gas exchange, respiration, and lung compliance. About 2% of all PF cases are due to mutations in the *SFTPC* gene, where missense changes are shown to produce a toxic protein causing alveolar injury. PF is also the most common reason for lung transplantation in North America and drug options for the condition slow progression, but do not stop or improve disease status.

Mutations in the SFTPB gene are associated with a rare, lethal condition, SP-B deficiency. This condition presents neonatally and is characterized by respiratory distress and neonatal death within the first weeks of life. Exogenous surfactant is the only treatment for SP-B deficiency, providing only a transient treatment and lung transplantation is the only cure for the condition.

Our lab has recently shown the potential of a novel viral vector gene therapy (AAV6.2-FF) for the treatment of a surfactant protein deficiency (SP-B deficiency), restoring expression of the *Sftpb* gene and extending the lifespan of SP-B deficient mice by over 300+ days compared to controls. Additionally, our lab has extended the use of this gene therapy platform for the treatment for *Sftpc*-related pulmonary fibrosis in a transgenic mouse model of the disease

(manuscript in review). Given optimization and further understanding of these models, these applications offer the potential for improved treatment of these surfactant protein conditions through the use of this novel gene therapy platform.

2.2 Hypothesis

Based on these findings, I firstly hypothesize that the application of this AAV-6.2-FF-*Sftpc* gene therapy may improve the condition of the L184Q model of *Sftpc*-related Pulmonary Fibrosis.

Additionally, I hypothesize that the characterization of the antibody response to the AAV6.2-FF vector in the previously established model of SP-B deficiency will allow for further understanding of the therapeutic and it's potential translation to clinic.

2.2 Objectives

My objectives in the model of L184Q mice are as follows: i) Characterize the L184Q phenotype at baseline. ii) Establish the injury model of bleomycin fibrosis in L184Q knock-in mice compared to the I73T model of disease. iii) Administer the AAV6.2-FF gene therapy to L184Q mice and assess feasibility of the technology transfer.

In the model of SP-B deficiency, my objectives are as follows: i) Assess longterm survival of adult mice who received AAV6.2-FF-*Luciferase in utero* ii) Re-administer the AAV gene therapy product in these mice as adults. iii) Quantify levels of serum antibodies following re-administration in adult mice to characterize the antibody response following adult administration. iv) Track longterm expression of AAV-*Luciferase in vivo*.

3. MATERIALS AND METHODS

Institutional approval for animal study

All mouse experiments performed in these studies were approved by the Animal Care and Veterinary Services (ACVS) Committee at the University of Ottawa under the protocol OHRI-1696. All of the experiments were performed in compliance with the animal guidelines of the Canadian Council on Animal Care following the ARRIVE guidelines[55].

Recombinant AAV plasmid generation and vector production

All work generating the final AAV6.2FF vector and the plasmid was completed at The University of Guelph by the Wootton Lab, with which we have collaborated throughout these experiments according to the published protocols[29].

In summary, the AAV plasmid consists of a CASI promoter of the human cytomegalovirus immediate early gene enhancer region, the chicken beta actin promoter, and the human ubiquitin C promoter, as well as the woodchuck hepatitis virus post-transcriptional regulatory element (WPRE) and simian virus 40 polyadenylation sequence downstream of the transgene with flanking adeno-associated virus 2 (AAV2) inverted terminal repeats (ITRs). The *Sftpc* transgene was synthesized and optimized using the murine sequence and GenScript. The AAV6.2FF vector was produced and quantified by the Wootton Lab at the University of Guelph by plasmid transfection of HEK293 cells. Vector genomes are quantified using TaqMan qPCR assay by targeting the inverted terminal repeat sequence of the AAV2 genome using the primers Forward: 5′–GGA ACC CCT AGT GAT GGA GTT–3′; Reverse: 5′ CGG CCT CAG TGA GCG A–3′; and Probe: 5′–FAM-CAC TCC CTC TCT GCG CGC TCG-BHQ – 3′.

Animal model

The following procedures were carried out at The Ottawa Hospital Research Institute and the University of Ottawa. In these studies, C57Black/6 mice were used containing the L184Q mutation in the *SFTPC* gene. These mice were initially generated by the lab of Dr. Timothy Weaver as described in the Journal of Clinical Investigation (Sitaraman et al, 2021). Mice were housed at the University of Ottawa ACVS facility on a 12h/12h off cycle and at room temperature of 21°C. Mice were maintained on regular mouse chow. All mice were caged in an open cage system. Up to 4 animals were housed per cage and grouped with littermates and by sex. Mice were assigned a numerical ID. The treatment of mice was randomly assigned. Animals in these studies were typically 8-10 weeks of age at the time of administration in each experiment. They were weighed regularly, before and during the experiment until the day of harvest. The negative control groups consisted of animals placed under anaesthesia and were injected with vehicle. Animals were monitored consistently throughout these studies and weighed daily following administration of bleomycin due to the harsh and unpredictable responses from these mice.

Animal Genotyping

To confirm mouse genotype, we used previously established protocols. We used the DNA extraction for PCR obtained from clipped ear or tail tissue using the AccuStart II Mouse Genotyping Kit (Quanta Biosciences) according to the manufacturer's instructions. The genotyping samples were then run on 5% agarose gels and imaged for quantification using the Molecular Imager Gel Doc XR system (Bio-Rad). Primer sequences for genotyping knock-in mice can be found in Table 1

Table 1. **Primer Sequences for Genotyping of L184Q Mice**. Sequence for each primer used to genotype each mouse, distinguishing between heterozygous and homozygous for the L184Q mutation.

Primer	Sequence
KI P1	TGG ACA TGA GTA GCA AAG AGG TC
KI P2-625	CCA TCT GTT GTT TGC CCC TC
KI P4	ATC CTA AAA GCC CAA TCC TAA GC

The following sets of primers were used for each the wildtype (WT) or knock-in (KI) mice:

WT (P1 - P4): 182 bp

KI allele (P2-625 - P4): 484 bp

Cycle protocol: The reaction mix consisted of the following at each given volume: 2.0X Apex Taq RED Master Mix with 1.5 mM $MgCl_2$ from Genesee Scientific, catalog #42-138. The precise reaction mix and PCR reaction protocol are specified in Table 2 and 3, respectively.

Table 2. Reaction Mix for L184Q Genotyping. Each reagent and volume for the genotyping of L184Q mice.*(Note: gDNA resolubilized in 10 mM Tris, pH 8-8.5)

Component	Volume
2X Apex Red Rxn Mix	10µl
P1 (10 pmole/µl)	1µl
P2-625 (10 pmole/µl)	1µl
P4 (10 pmole/µl)	1µl
Water	6µl
gDNA	1µl*

Table 3. PCR Protocol for Genotyping of L184Q mice.

Temperature	Time	Cycles
94˚C	120s	
94˚C	30s	30x
55˚C	30s	
72˚C	60s	
72˚C	180s	
4˚C	¥	

Oropharyngeal administration

Oropharyngeal administration was used for the SP-C-LQ experiments. Prior to oropharyngeal administration, mice were anaesthetized using isofluorane (Fresenius Kabi). The mouse respiration was monitored visually throughout isofluorane administration until mice were

bradypneic. When they were deeply anesthetized, breathing slowly from the abdomen for a count of 10, they were placed on a vertical support (Harvard Apparatus) and suspended by their upper incisors using surgical thread. The ventral side of the mouse was positioned facing away from the operator and the tongue was gently pulled out using forceps. The airway was assessed in order to visualize the trachea. A 200 µL pipette containing the 50 µL of the AAV vector to be delivered was placed in the oral cavity of the mice and the volume was administered. Mice remained on the apparatus for approximately 15 seconds, or until breathing began to speed up. Mice were then removed from the apparatus and left to recover in an incubator for 15-30 minutes. Mice were monitored within 3 hours following the procedure to ensure proper recovery.

Tracheal Intubation Administration

Tracheal intubations were conducted as part of the SP-B deficiency experiments. Intubations were done based on previously established protocols in our lab. Briefly, mice were subcutaneously injected with 1 mL of saline to prevent dehydration throughout the procedure. Mice were then anesthetized intraperitoneally (IP) with 100 mg Ketalean (Ketamine; Bimeda-MTC Animal Health Inc) per 10 mg Rompun (Xylazine; Bayer Inc) per kg of body weight. Gel for the eyes of the mice (CLC Medica) was then applied to protect against corneal drying due to the length of the recovery period. Once fully anesthetized, the mouse was placed on a vertical support (Harvard Apparatus) and suspended by its upper incisors using surgical thread. The ventral side of the mouse was positioned facing away from the operator and the tongue was gently pulled out using forceps. Mice were then intubated with a catheter (BD Insylte) into the trachea. To visualize the tracheal opening, a light source was positioned shining onto the ventral side of the mouse, projecting light into the cavity. Once the catheter was properly visualized and positioned in the trachea, a 1 mL syringe containing 50 to 60 µL of AAV vector was

administered through the catheter. This was followed by three 100 µL injections of air with the 1 mL syringe, in an attempt to improve AAV distribution throughout the distal lung. The mouse was left in this standing or upright position to allow time for vector dispersion throughout the lungs. Mice recovered in a 37 °C incubator post-surgery for 1-2 hours and were monitored for breathing and movement throughout this period.

Lung function analysis

Lung function including a measure of pulmonary surfactant function was calculated following the generation of individual pressure-volume (PV) curves for each mouse as previously described[56,57]. Briefly, mice were euthanized with an intraperitoneal injection of Euthanyl (Pentobarbital Sodium Injection; Bimeda-MTC Animal Health Inc). Within 10 to 15 min of Euthanyl injection, pressure-volume curves were obtained using a small animal mechanical ventilator (flexiVent, Scireq). A cannula attached to the flexiVent was secured to the trachea of euthanized animals in a supine position. The lungs were inflated with regular increasing intervals of pressure to a maximum of 30 cmH_2O. Lungs were subsequently deflated with regular decreasing intervals of pressure to obtain pressure-volume curves. All data were obtained using the flexiWare version 7.0 (Scireq) software. Pressure-volume curves were normalized to the body weight of each animal[58]. Measurements including %V10, Peak Inspiratory Pressure (PIP), residual volume (RV), lung compliance and elastance were extracted from the pressure-volume curves according to previous protocols[5]. Briefly, PIP is the volume at the defined maximal pressure of 30 cmH2O. The compliance is the slope at any linear region of the deflation curve and was calculated by the ratio in the change in volume between 10 cmH2O and 7 cmH2O (ΔV) over the change in pressure (ΔP). Elastance is calculated as the inverse of compliance.

Serum Collection from Lateral Saphenous Vein & Blood Processing

Mice were extracted from their cage and placed in restraint tubes with hind legs exposed. Serum was collected from the lateral saphenous vein of SP-B mice using a 23-gauge needle by introducing a small prick to the lateral saphenous vein. Using a blood collection tube, a small amount (maximum 1mL) of blood was collected from mice and they were left to recover in their cages. In the survival study, blood was collected at 3 days before (−3D), and 1 (+1D), 7 (+7D), and 29 days (+29D), and 60 days (60D) after AAV administration.

Blood samples from mice were processed immediately following collection. Blood collection tubes were centrifuged at 4˚C for 10 minutes to separate the serum and plasma phases. Serum from each sample was then extracted using a 10uL pipette and placed in a 1.5mL centrifuge tube and put on ice. Samples were stored at 4˚C for immediate use and -20˚C for storage.

ELISA Detection for AAV6.2-FF Antibody

A 96-well plate was coated in a solution of 1e10 vg/ml AAV6.2FF-mCherry in PBS and 30 ul of this prepared solution was added to each well. The plate was sealed and stored at 4˚C overnight. The coating solution was decanted and washed with 100 ul of PBS 0.2% Tween-20 3 times. Blocking buffer was added to each well. A1:40 dilution of mouse serum collected to blocking buffer was prepared in separate tubes. Proceeding dilutions of 1:400 were made prior to transferring to the plate. The plate was serially diluted by 1:2 directionally towards the negative wells at the end. Samples were run in duplicates and new pipette tips are applied when moving between rows. The ADK6 positive control was diluted to 1:400 and then applied to the 96 well plate. The plate was sealed and store at 37˚C for 1hr. The plate was decanted and washed 3 times with 100 ul of PBS 0.2% Tween-20. A secondary antibody solution was made up as a master mix at 1:2000 ratio of goat-anti-mouse horse radish peroxidase antibody and blocking buffer and applied to the plate. This was then sealed and incubated at 37˚C for 1hr. The secondary antibody

mixture was decanted, and the plate was washed 3 times with PBS 0.2% Tween-20. Equal parts of the TMB solutions were mixed and 30 ul of this prepared solution was applied to each well and incubate for 15 minutes on a shaker at room temperature. The plate was read at 600 nm with the Glomax multi-detection system.

RNA extraction and dosage

Right lungs snap frozen and stored in -80 were placed on dry ice and subsequently cut into small sections. A weight of ~30mg was weighed and placed in a 2 mL tube placed on ice. Using a 5mm stainless steel beed and lysis buffer RLT (Qiagen), lungs were then mechanically digested using the Tissue-Lyser II machine (Qiagen) for 1 minute 30s, twice at 25 Hz. After mechanical and chemical digestion, beeds were removed and homogenized tissue was placed in a new tube and centrifuged at 15 000 RPM for 3 minutes. The liquid supernatant was used in the Qiagen RNA-Easy Extraction Kit (#74104) according to manufacturers instructions. RNA levels were measured directly using the NanoDrop One Microvolume UV-Vis Spectrophotometer (ThermoFisher). The samples were then stored at -20°C.

RT-qPCR

Sftpc, *SFTPC*, *Gapdh* were reverse-transcribed with the iScript Reverse Transcription Supermix for RT-qPCR Kit (Biorad) using 500ng of RNA. qPCR was performed using the CFX96 Touch Real-Time PCR Detection System and TaqManTM technology. For relative quantification, miRNA and RNA levels were calculated using the $2^{-\Delta Ct}$ method and normalized to the expression levels of *Gapdh*. Each sample was assessed in triplicate.

Protein extraction and dosage

Snap frozen, right lung samples were removed and a section of the lung was cut and placed in a 2mL tube to be mechanically and chemically digested. This was done using a 5mm stainless steel

beed in 700 µL of PBS, 1% Protease inhibitor, and 1X Phosphatase Inhibitor. Tubes were placed on ice and homogenized using the TissueLyser II machine (Qiagen) for 1 minute 30s, twice at 25Hz. Supernatant was removed and placed in a new vial for storage at -20°C.

Protein concentration was done using a BSA protein standard in a 96 well plate in triplicate. Each sample was run in triplicate and protein breakdown mixture was used as a blank. Bradford Reagent (BioRad) was used to determine the protein concentration and concentrations were quantified using the Gen5 software at 595nm. Values were extracted and analyzed.

Western blot

30µg of total protein was extracted and heated for 5 minutes with beta-mercaptoethanol. Total protein mix was then size separated on 10-20% Tricine gels and transferred to iBlot2 nitrocellulose membranes (Fisher). The membrane then underwent of blocking in milk-TBST. Membranes were then incubated with primary antibody overnight at 4˚C (see Table 4). They were then incubated with secondary antibody. Each incubation was approximately 1 hour and the membranes were washed 3 times for 5 minutes with a 0.05% TBS-T solution. ß-actin was used as the housekeeping protein for each gel. The membranes were then imaged and quantified using the Bio-Rad ChemiDoc.

Table 4. Antibodies for Western Blot. Each primary antibody used for various Western blot assays completed.

Antibody	Company and ID	Concentration Used
ß-actin	ß-actin Monoclonal Rabbit antibody Cell Signaling Technology #4967	1:1000
Bax	Bax Monoclonal mouse antibody, Proteintech #CL488-6026	1:1000
Nrf2	Mouse surfactant protein C, Santa Cruz Biotechnology	1:1000
NOX2	NOX2 polyclonal antibody, Proteintech #19013-A-AP	1:1000
NOX4	NOX4 Polyclonal antibody, Proteintech #143147-1-A	1:1000
Secondary Antibody	Goat anti-Mouse IgG (H+L) Secondary Antibody, HRP Invitrogen #62-652	1:5000

H&E staining, MLI & fibrosis score

The left lungs of mice were set in 10% formalin following harvest and placed in 70% EtOH 48h later. Lungs were then sent to the Louise Pelletier Histology Core at the University of Ottawa for processing, embedding, sectioning, and staining. Samples were stained with hematoxylin and eosin (H&E) and were assessed using the mean linear intercept and fibrosis score.

Mean Linear Intercept (MLI) represents the measure of the average diameter of thew alveolus and was used to determine gas exchange efficiency. MLI was measured using the Quorum Analysis software and used in a semi-automated fashion. The software uses a 155.34µm lined grid and moves across sections in randomized intervals, called fields of view (FOV). The number of intersections between the line and the alveolus with the parenchyma is quantified. The formula used is as follows: [MLI=(FOV x 155.34*I*); where FOV represents the number of fields of view counted and *I* represents the number of intersections quantified across the 155.34µm line]. For each sample, 4 sections were assessed and approximately 200 FOVs were quantified in each.

The fibrosis score, or Ashcroft Hübner (AH) score is a method of quantitative histological scoring for lung samples in small animal models. This score is used to represent the amount of fibrosis detected in a histological sample. To obtain the AH score, 1-2 H&E stained sections were used per sample. From each section, a randomized number of FOVs were assessed when lung tissue was present in >50% of the FOV. Each eligible FOV was then scored on a scale from 0-8 based on the previously established criteria in Hübner et al, 2008 based on the extent of fibrosis present. To calculate the AH score, a weighted average was calculated and summed.

In-Utero Administration

All *in-utero* administration surgeries were perform by Liqun Xu of the XPlore Lab. Female mice from the inducible model of SP-B deficiency were maintained on doxycycline and bred with male SP-B deficient mice maintained on doxycycline. On D16 of pregnancy, female mice were sedated using Ketamine-Xylazine and a vertical midline incision was performed. The uterus was exposed and using a 30G needle was used to inject Luc-AAV6.2FF at a concentration of 10^{11} vg/mL. The injection was performed around the mouth of the pups to optimize lung expression.

Statistical Analysis

Graphpad Prism 8 software was used to perform all statistical analyses. Means are represented with standard error of the mean error bars. If the experiment consisted of a 2-group comparison, statistical analysis was by the 2-tailed Student's t-test. If the experiment consisted of 3 or more comparison groups, the statistical test used was ordinary one-way ANOVA with Tukey's multiple comparisons post hoc test. Kaplan Meier survival curves were analyzed with the Log-rank, according to GraphPad Prism standard analyses. Serum antibody measurement data were analyzed by fitting the Mixed Effects Model with Tukey's multiple comparison post hoc test. P-values less than 0.05 were considered significant.

4. RESULTS

Chapter I – Comparison of the *Sftpc*-173T-fibrosis model to the L184Q mutation

4.1 Establishing L184Q baseline measurements

L184Q (LQ) mice and age-matched, wildtype control mice (C57Bl/6) were housed in room air from birth. Mice were left to age until 9 weeks postnatally and bodyweight (g) was monitored every other day for 17 days (Figure 3A). LQ mice demonstrated a significant reduction in *Sftpc* expression compared to wildtype (WT) mice (Figure 4A). A significant increase in proSP-C protein and a reduction in matureSP-C (mSP-C) was observed in LQ mice when compared to controls, indicating accumulation of the proSP-C protein in LQ mice as expected (Figure 4C, D). Histologically, LQ mice did not show an increase in the MLI compared to WT mice. This indicates no structural change between L184Q and WT mice. The Ashcroft-Hübner (AH) score for pulmonary fibrosis revealed no difference in the LQ mice when compared to both I73T and WT mice, indicating no spontaneous fibrotic phenotype at baseline (Figure 5).

The characterization of the baseline L184Q phenotype revealed a comparable overall phenotypic pattern to the I73T mouse model. L184Q mice demonstrated no significant change in lung structure compared to the I73T mice.

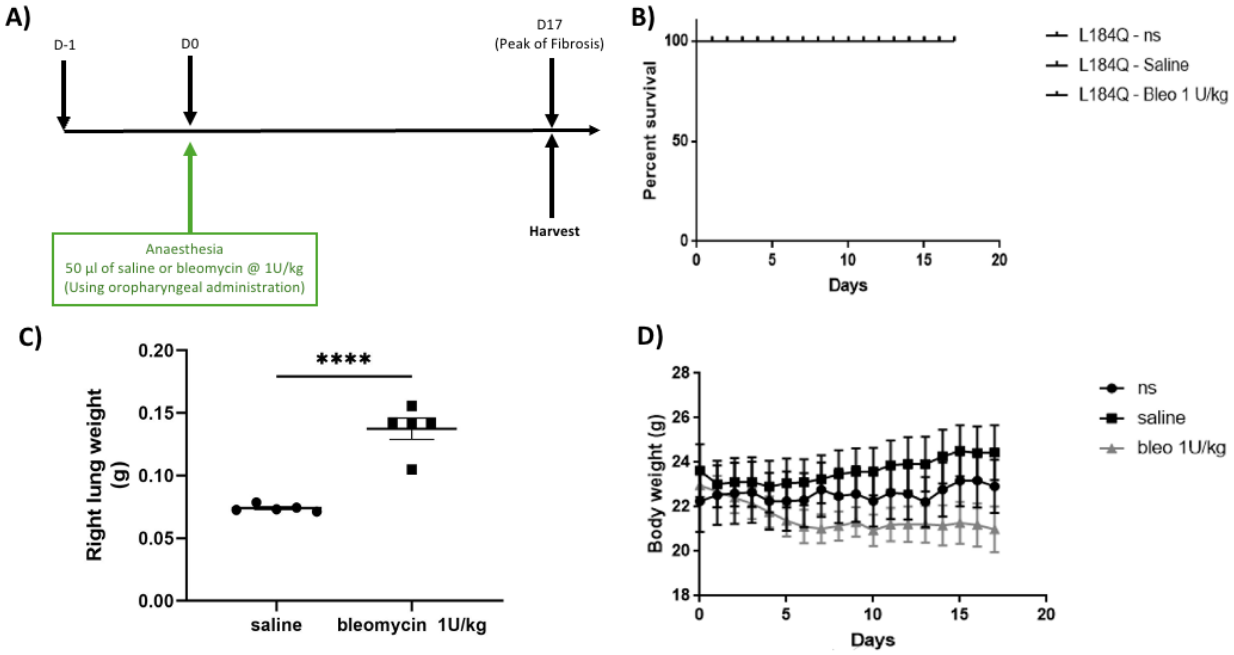

Figure 3. Baseline characterization of LQ mouse model of bleomycin fibrosis. **A)** Experimental outline. Animals either underwent oropharyngeal administration with saline (n=6), bleomycin (1U/kg, saline vehicle) (n=6), or no treatment (n=6) and were harvested at D17 after administration. **B)** Percentage survival of entire cohort. C) Right lung weight (g) between saline and bleomycin mice. **D)** Body weight (g) tracked over time between all treatment groups. Values are represented as mean ± SEM. P values were calculated using the student's t-test. Significant results are shown as *P ≤ 0.05, **P ≤ 0.01, ***P ≤ 0.001, and ****P ≤ 0.0001

4.2 Establishing a model of injury by bleomycin-induced fibrosis

Upon characterizing the baseline measurements of LQ mice, the previously established model of bleomycin-induced fibrosis was applied. LQ mice and age-matched WT mice were randomized into bleomycin or saline groups and each administered the respective agents at 9 weeks of life. Bleomycin (1U/kg) or saline was administered by oropharyngeal administration and bleomycin-treated groups were found to have significantly higher right lung weight (RLW), indicating the accumulation of tissue and fibrosis in the lungs (Figure 3C). No significant changes in bodyweight was observed between groups (Figure 3D). At the mRNA level, LQ mice maintained significantly lower levels of *Sftpc* expression with bleomycin treatment. Bleomycin treatment was not observed to change *Sftpc* expression in WT mice (Figure 4A, B). LQ-bleomycin mice also maintained a significantly higher amount of proSP-C and reduced levels of mSP-C compared to WT-bleomycin group, maintaining the previously established molecular phenotype observed in LQ mice (Figure 4C, D). The MLI and AH score were both significantly increased upon bleomycin administration in LQ mice compared to the saline group (Figure 5A, C). Functionally, a significant decrease in PV-loop was observed in the LQ-bleomycin group compared to the saline group, indicating a functional difference in the respiration of bleomycin treated mice (Figure 6A). However, no other functional measurements displayed changes in the LQ-bleomycin mice, which strays from the expected result.

Altogether, these findings indicate an injurious effect in the LQ-bleomycin model, successfully applying our previously established protocol for pulmonary fibrosis.

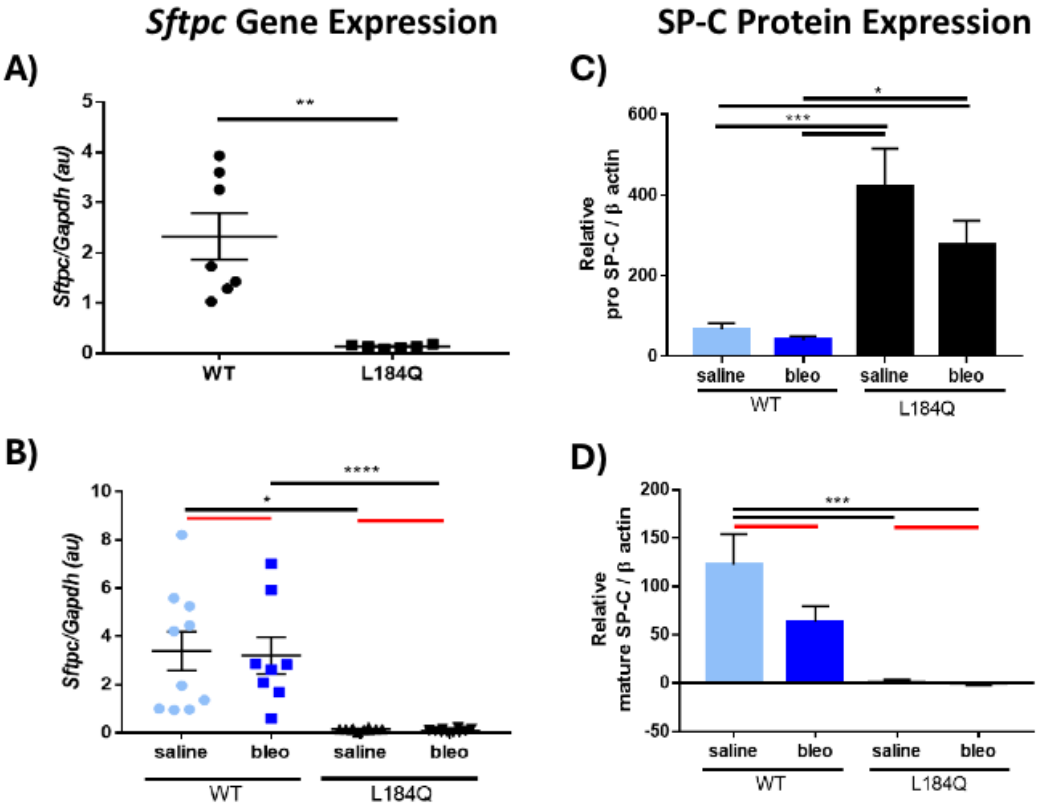

Figure 4. Gene and protein expression with bleomycin administration. A) Endogenous *Sftpc* expression levels in wildtype (n=7) and L184Q (n=6) mice. **B)** *Sftpc* expression levels in wildtype (n=10) mice and wildtype mice with bleomycin (n=8) quantified by RT-qPCR. Expression levels of endogenous *Sftpc* in L184Q mice administered saline (n=8) or bleomycin (n=8) quantified by RT-qPCR. **C) & D)** Levels of pro- and mature SP-C protein in WT and LQ mice administered saline or bleomycin, quantified by Western blot and imaged with ChemiDoc. Values are represented as mean ± SEM. P values were calculated using the student's t-test (A) and one-way ANOVA with Tukey's multiple comparisons test (B, C, D) Significant results are shown as *P ≤ 0.05, **P ≤ 0.01, ***P ≤ 0.001, and ****P ≤ 0.0001

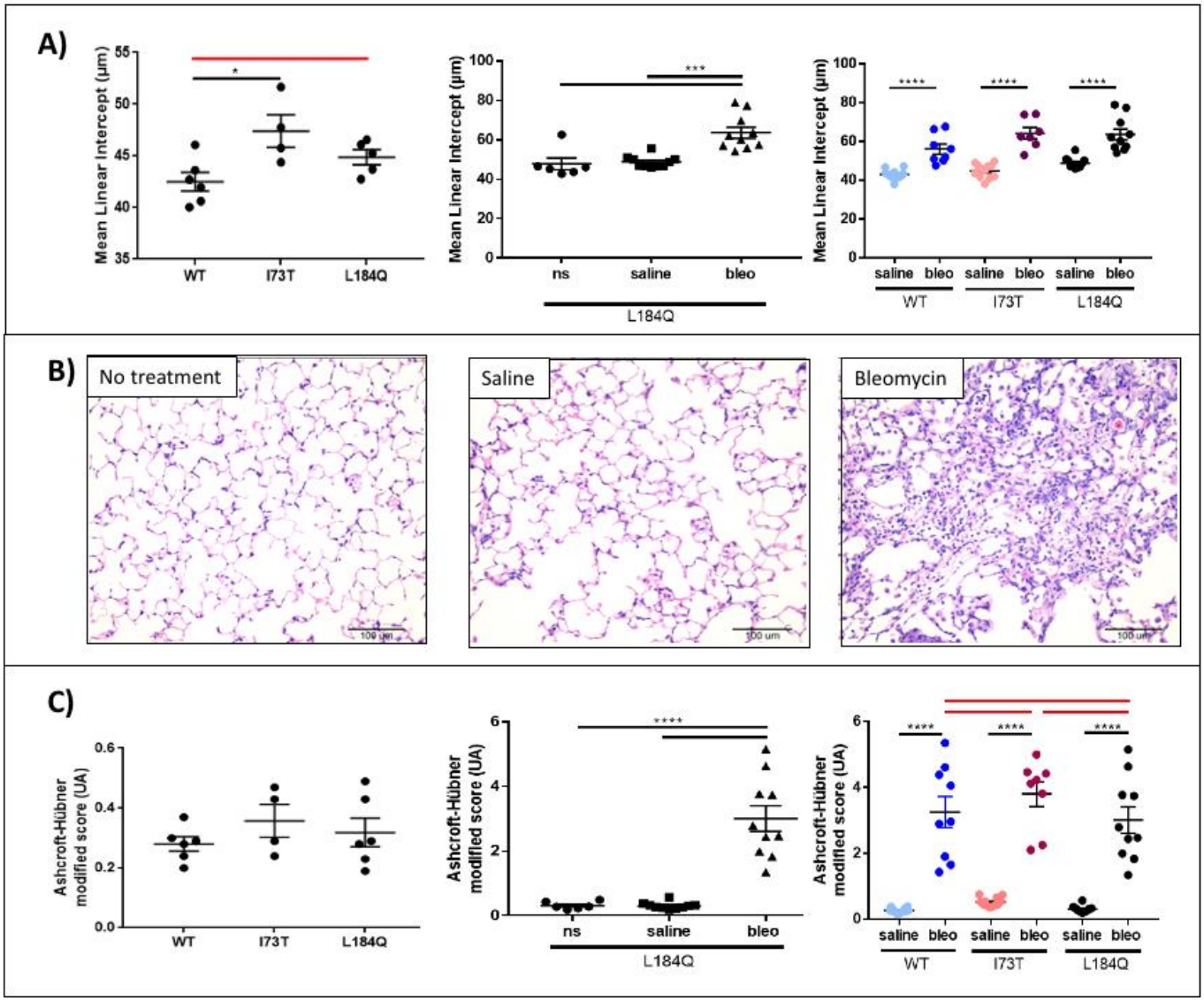

Figure 5. Histological analyses of LQ lungs with bleomycin injury. A) *Left panel* – Baseline measurement of Mean linear intercept (MLI) of wildtype (WT), I73T, and L184Q mice with no treatment. *Middle panel* – Mean linear intercept of LQ mice administered no saline (ns), saline, or bleomycin (bleo). *Right panel* – Comparison of the Mean linear intercept between WT, I73T, and L184Q mice administered bleomycin or saline. **B)** Representative, H&E stained, histological images of L184Q mice administered no treatment, saline, and bleomycin (respectively from left to right). C) Comparisons of Ashcroft-Hubner score for WT, I73T, and L184 animals with various treatments. Values are represented as mean ± SEM. P values were calculated using the one-way ANOVA with Tukey's multiple comparisons test. Significant results are shown as *P ≤ 0.05, **P ≤ 0.01, ***P ≤ 0.001, and ****P ≤ 0.0001.

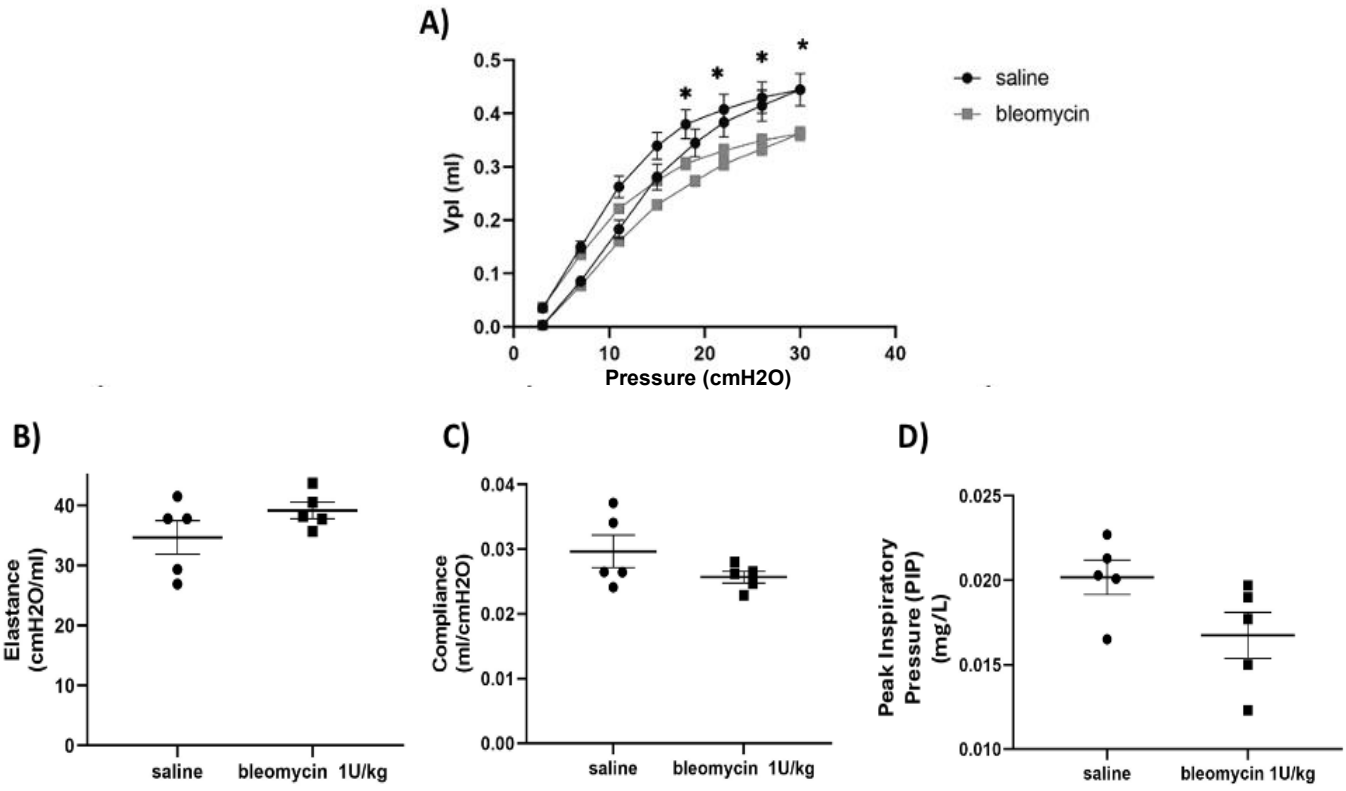

Figure 6. Lung function analyses of LQ mice administered bleomycin. A) Pressure-Volume loops extracted from lung function tests performed with FlexiVent machine in comparing LQ mice treated with vehicle (saline) or bleomycin (1U/kg) (n = 5; n = 5)**. B), C), D)** Measures of lung function extracted from the Pressure-volume loops: elastance (B; cmH2O/ml), compliance (C; ml/cmH2O), Peak inspiratory pressure (D; mg/L). Values are represented as mean ± SEM. P values were calculated using the student's t-test except in PV loop, which used the two-way ANOVA with Tukey's multiple comparisons test. Significant results are shown as *P ≤ 0.05..

4.3 Investigating inflammation pathways in LQ mice

With observations of the LQ model differing from the I73T model and reports of oxidative stress (OS) in LQ mice, we investigated the presence of inflammation and apoptotic activity in LQ mice. LQ mice were randomized into no treatment, vehicle (saline), and bleomycin (1U/kg) groups. Each treatment was administered according to the previously established protocol by oropharyngeal administration at 9 weeks old and mice were collected D17 post-injection in order to capture the peak of fibrosis by bleomycin.

LQ mice were observed to have significantly low levels of *Bax* gene expression in no treatment and saline groups when compared with both WT and bleomycin groups (Figure 7A). Additionally, bleomycin treated animals demonstrated increased *Bax* expression compared to other LQ mice, but no significant difference was detected between bleomycin and WT groups. Bax protein levels also demonstrated a significant increase upon the administration of BLM. All LQ mice, regardless of treatment demonstrated significantly low levels of gene expression in *Nox4* and *Nfe2l2* markers. Levels of the Nfe2l2 (Nrf2) protein also reflected this pattern. However, no change in protein levels of the Nox4 marker was observed at significant levels. LQ mice treated with bleomycin demonstrated significantly higher *Nox2* gene expression compared to all other groups, indicating the role of *Nox2* in the development of bleomycin-fibrosis. This change was also reflected in the levels of *Nox2* protein detected (Figure 7B, D). Altogether, these findings may indicate an inflammatory and apoptotic phenotype in the L184Q mice.

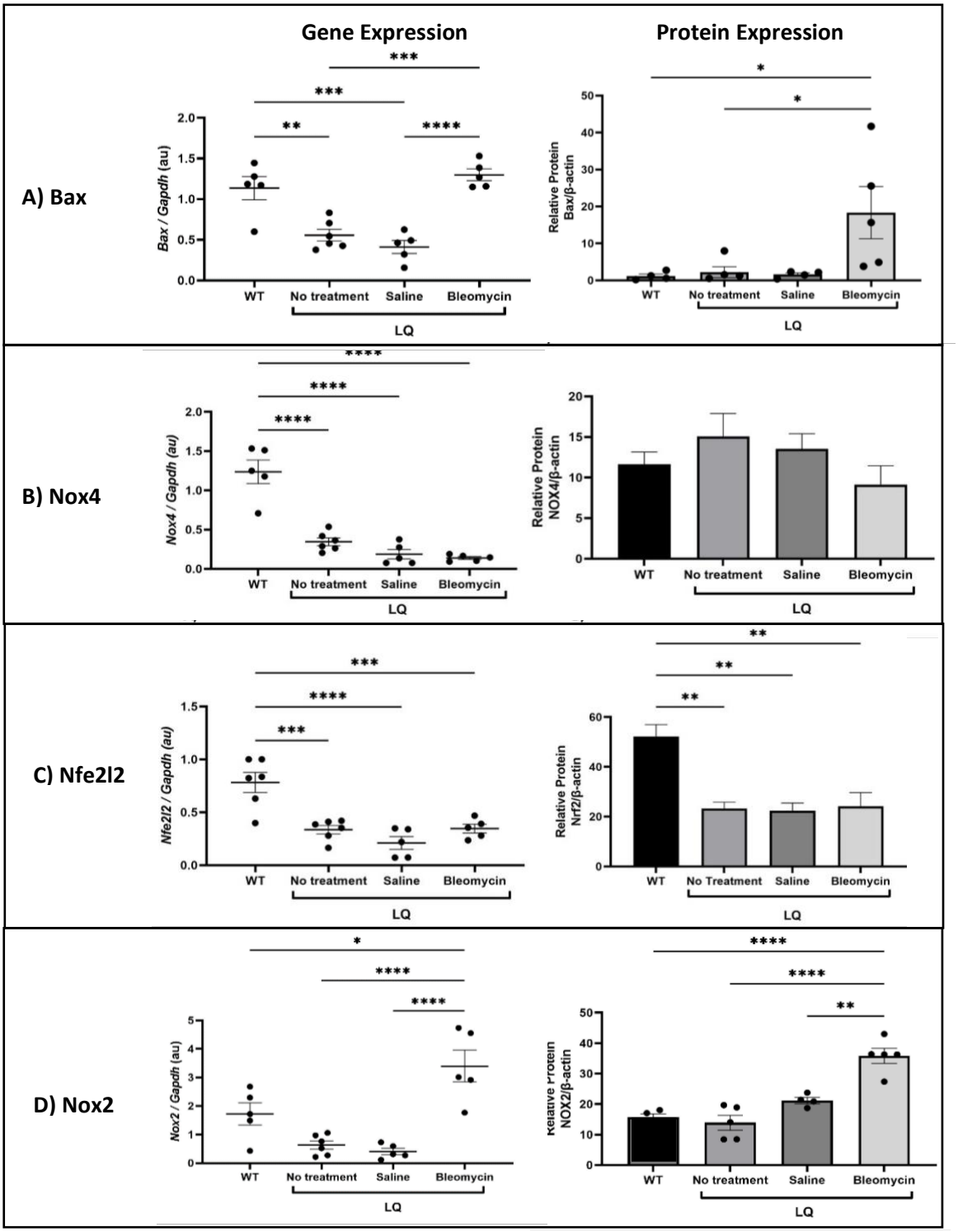

Figure 7. Markers of inflammation and apoptosis in LQ mice. Left panels represent gene expression levels by RT-qPCR. Right panels representing protein levels by Western blot. Measure of inflammation in WT and LQ animals with no treatment, saline, or bleomycin (n = 5 per group). Values are represented as mean ± SEM. P values were calculated using the two-way ANOVA with Tukey's multiple comparisons test. Significant results are shown as *P ≤ 0.05, **P ≤ 0.01, ***P ≤ 0.001, and ****P ≤ 0.0001.

4.4 Piloting an anti-inflammatory approach for the LQ model

Preliminary experiments were carried out administering AAV6.2-FF by another member of the lab, which demonstrated an inflammatory response identified by immune cell infiltration. Histological analysis of the experiment revealed inflammation in LQ mice administered AAV gene therapy yielding an adverse effect. Additionally, following investigations which indicated a potential increase in oxidative stress and inflammation in LQ mice, an anti-inflammatory and anti-fibrotic drug, Nintedanib, was piloted in LQ mice. A repeat of the treatment with the AAV vector was performed in a side-by-side manner with Nintedanib in order to reassess potential inflammation previously observed with administration. 9-week-old LQ mice were randomized into the following groups: vehicle, AAV-GFP, AAV-murine-*Sftpc*, and Nintedanib. Age-matched WT mice were used as comparison (n = 6). Mice were administered the respective treatment on D0 via oropharyngeal administration. The Nintedanib group was administered the drug (25mg/kg) every other day for 10 days, adapted from previously published protocols. Bodyweight was measured throughout the 28-day experiment and no differences were observed (Figure 8A). No change in RLW was observed with Nintedanib administration or AAV6.2-FF administration (Figure 8A). No changes were observed in any measures of lung function between LQ mice and WT mice in all groups (Figure 8B). At a gene expression level, mice administered AAV6.2-FF demonstrated notable expression of the optimized *Sftpc* codon delivered indicating the successful delivery of the AAV vector and subsequent expression in the lungs (Figure 9A).. However, no significant change in gene expression was detected in all markers of inflammation or apoptosis (*Bax*, *Nfe2l2*, and *Nox2*). Future experiments may assess trends. At the protein level, expected trends were observed in LQ mice, demonstrating higher levels of proSP-C and low levels of mSP-C in untreated mice (Figure 10A). Additionally, the AAV-mSPC group showed

higher levels of mature SP-C protein, indicating successful administration of the AAV6.2-FF gene therapy, given the ability of the ATII cells to process the SP-C protein (Figure 10B). A significant increase in Bax protein levels was observed in LQ mice treated with AAV-GFP and AAV-mSPC compared with LQ mice administered saline which may indicate an increase in apoptosis given AAV delivery. Histologically, no significant change in AH score was detected between AAV treatment groups and non-AAV groups, although a wide variability was detected.

Based on these findings, no significant pattern of inflammation or oxidative stress was detected in LQ mice due to the AAV vector. However, trends in this direction may warrant further investigation. Additionally, a dose-response for the use of Nintedanib may be beneficial. Further characterization of both the LQ response to AAV6.2-FF and Nintedanib are required to better understand a possible treatment approach for the condition in the LQ mouse model of disease, however previous reports of widespread inflammation were not replicated.

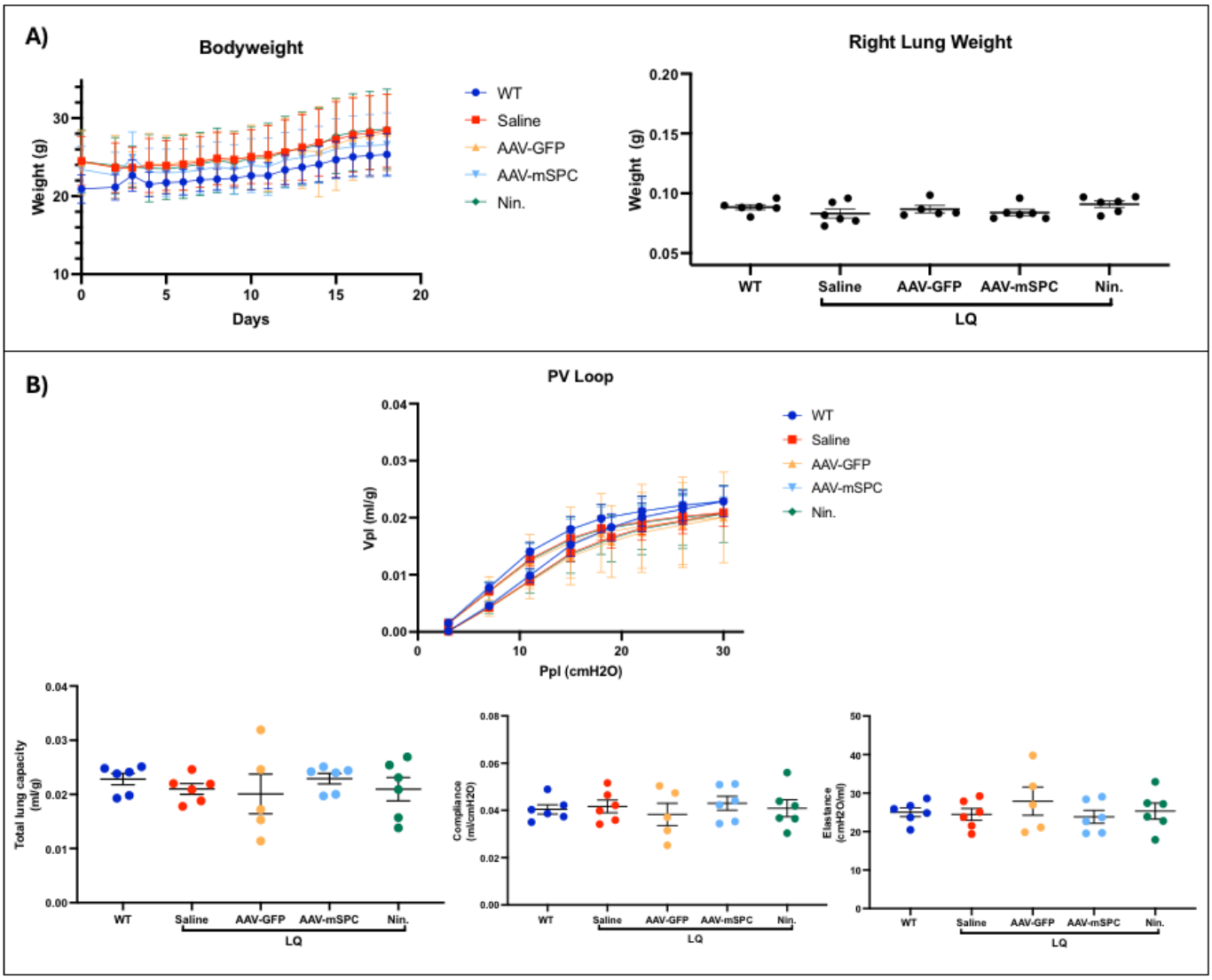

Figure 8. Lung function and baseline health of LQ mice with AAV6.2-FF re-administration and Nintedanib pilot. A) Bodyweight measurement and Right Lung Weight (RLW) comparisons of WT (n = 5), LQ-saline (n=6), LQ-AAV-GFP (n = 5), LQ-AAV-mSPC (n=6), Nintedanib (Nin.) (25mg/kg) (n=6). **B)** Pressure-Volume loops extracted from lung function tests performed with FlexiVent machine in comparing LQ mice treated with vehicle (saline) or bleomycin (1U/kg) (n = 5; n = 5)**.** Measures of lung function extracted from the Pressure-volume loops: elastance (cmH2O/ml), compliance (ml/cmH2O), Peak inspiratory pressure (mg/L). Values are represented as mean ± SEM. P values were calculated using the student's t-test except in PV loop, which used the two-way ANOVA with Tukey's multiple comparisons test. Significant results are shown as *P ≤ 0.05, **P ≤ 0.01, ***P ≤ 0.001, and ****P ≤ 0.0001.

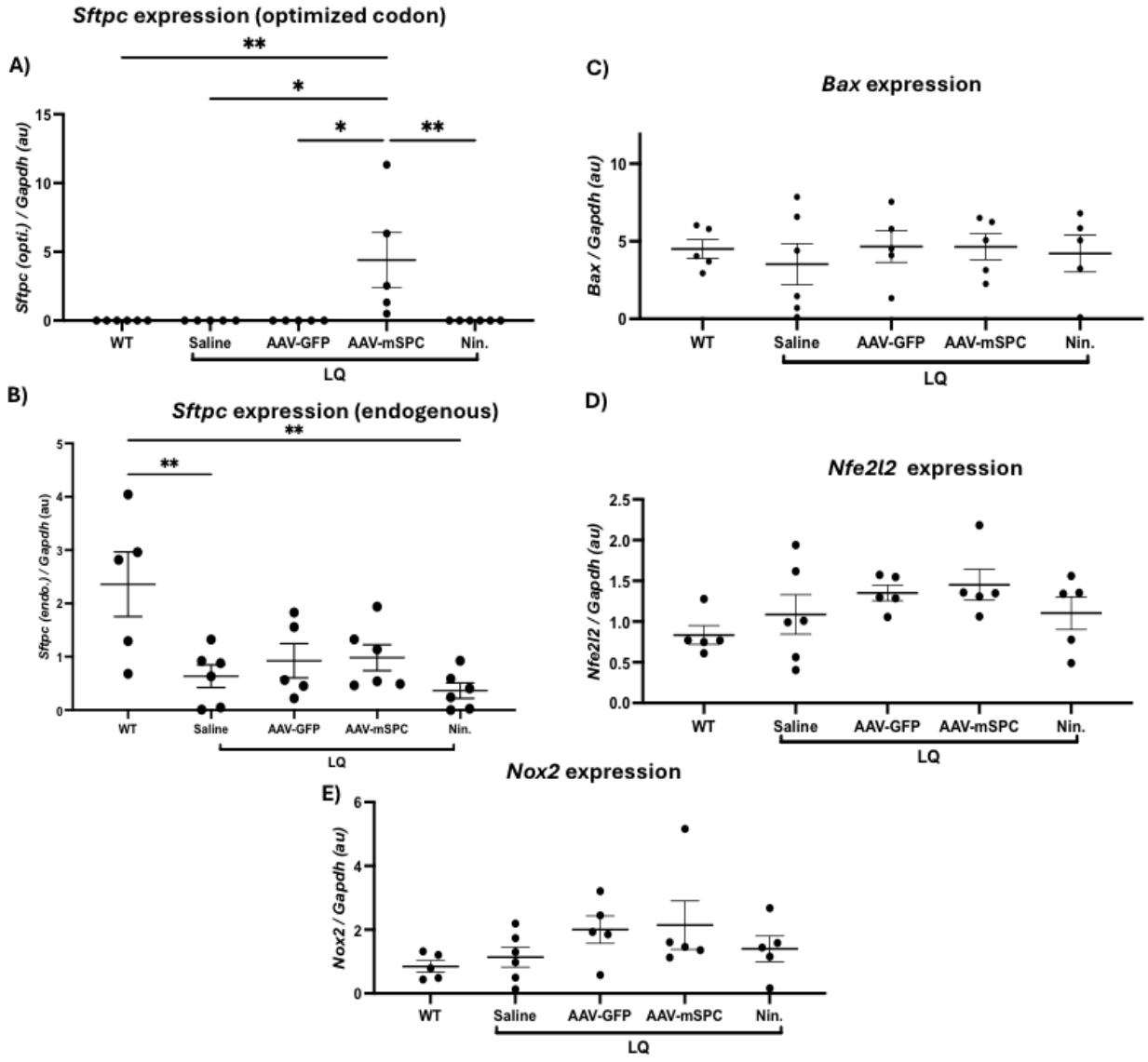

Figure 9. Gene expression levels of of inflammation markers in mice administered AAV6.2-FF and Nintedanib. Gene expression quantified by RT-qPCR in WT (n = 5) and LQ mice administered saline (n = 6), AAV-GFP (n = 5), AAV-mSPC (n = 6), and Nintedanib (Nin.) (n = 6) collected at D28. Values are represented as mean ± SEM. P values were calculated using two-way ANOVA with Tukey's multiple comparisons test. Significant results are shown as *P ≤ 0.05, **P ≤ 0.01, ***P ≤ 0.001, and ****P ≤ 0.0001.

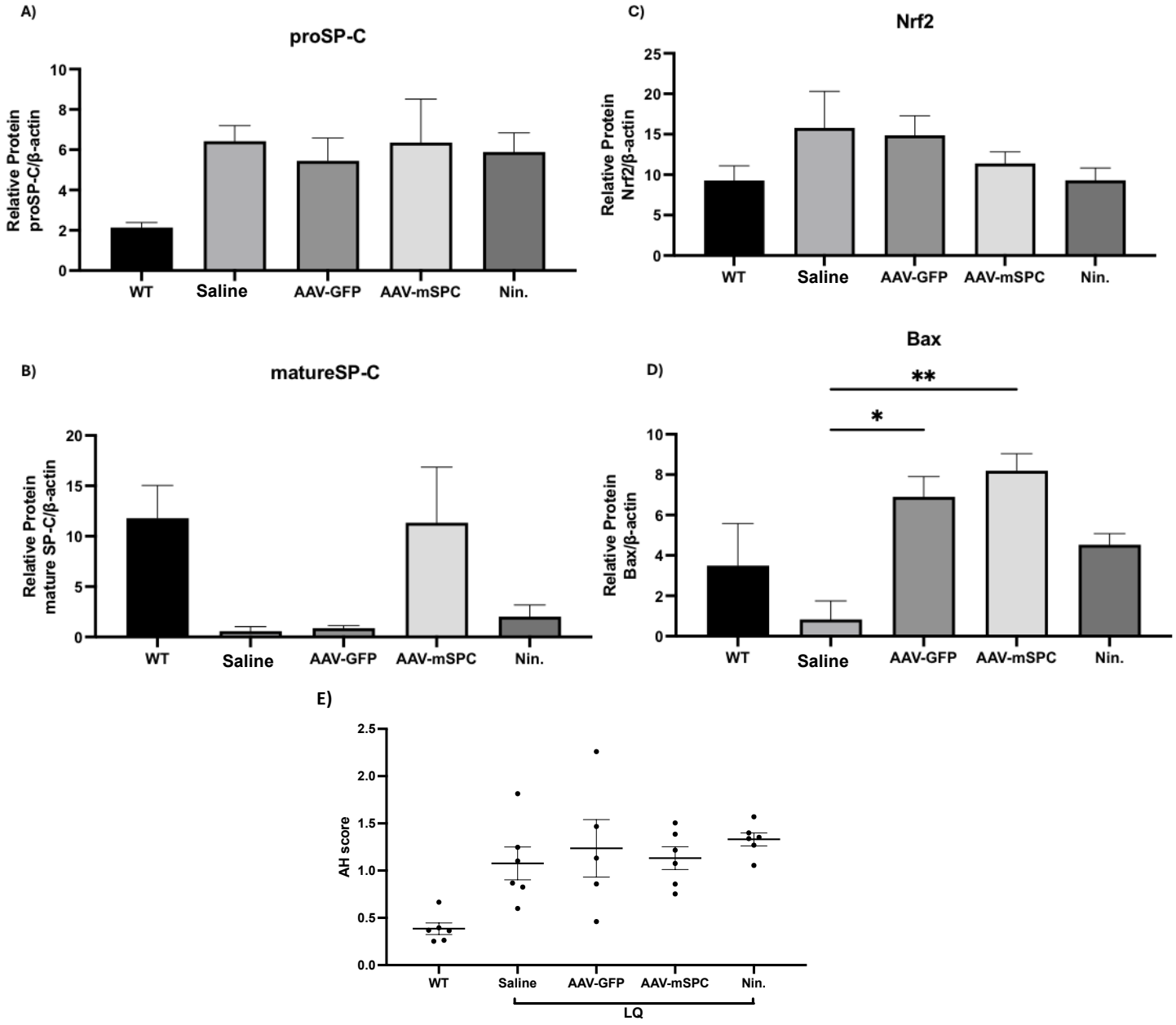

Figure 10. Presence of inflammation in mice administered AAV6.2-FF and Nintedanib. Protein levels relative to ß-actin quantified by Western blot in WT (n = 5) and LQ mice administered saline (n = 6), AAV-GFP (n = 5), AAV-mSPC (n = 6), and Nintedanib (Nin.) (n = 6) collected at D28. Values are represented as mean ± SEM. P values were calculated using one-way ANOVA with Tukey's multiple comparisons test. Significant results are shown as *P ≤ 0.05, **P ≤ 0.01, ***P ≤ 0.001, and ****P ≤ 0.0001

Chapter II – Longterm monitoring and assessment of AAV6.2-FF re-administration in SP-B mice injected *in-utero* with AAV6.2-FF

4.5 Re-administration of AAV6.2-FF in adult mice following *in-utero* administration.

Previously, two litters of mice under the control of a doxycycline (dox) dependent promoter in our model of SP-B deficiency (8 total) were injected *in-utero* with the AAV6.2-FF vector to assess in-utero injection as a potential method for administration, aiming to better recapitulate the clinical scenario more closely. In order to assess the antibody response to our AAV vector given *in-utero* exposure, mice were re-administered the AAV6.2-FF vector (10^{11} vg/mL) containing a Luciferase reporter gene by tracheal intubation twice throughout adulthood (D456 and D583). To characterize the health and antibody response of these mice which received AAV6.2-FF in-utero, survival, bodyweight, and serum antibody levels to AAV6.2-FF were collected. Bodyweight was measured daily beginning on D-7 leading up to re-administration and weekly following. Saphenous vein collection of serum was performed on D-3, D-1, D1, D3, and D7. Data was collected until ethical endpoint was reached. A control cohort of 4 mice who received gene therapy in-utero, but were not re-administered as adults were used.

Survival was measured beginning post-administration day 1. No significant changes in survival were detected given multiple re-administration of the AAV6.2-FF-*Luc* (Figure 11). No significantly different bodyweight was detected throughout the injection period. Serum antibody levels were minimal, but detectable prior to re-administration, indicating low levels of the AAV6.2-FF antibody is present from *in-utero* injection (Figure 11). Following first re-administration, serum antibody levels showed some levels of modulation, detected by a minimal rise on D7 post administration. However, one spike in M863 was detected prior to endpoint. Given a second re-administration of the vector, mice experienced a spike in antibody levels as

expected. Taken together, these findings may indicate *in-utero* injection of the AAV6.2-FF vector does not drastically change the expected antibody response, as previous literature indicates that multiple exposures increase antibody levels. These findings contribute to the characterization of the anti-body response with *in-utero* injection of the AAV6.2-FF vector.

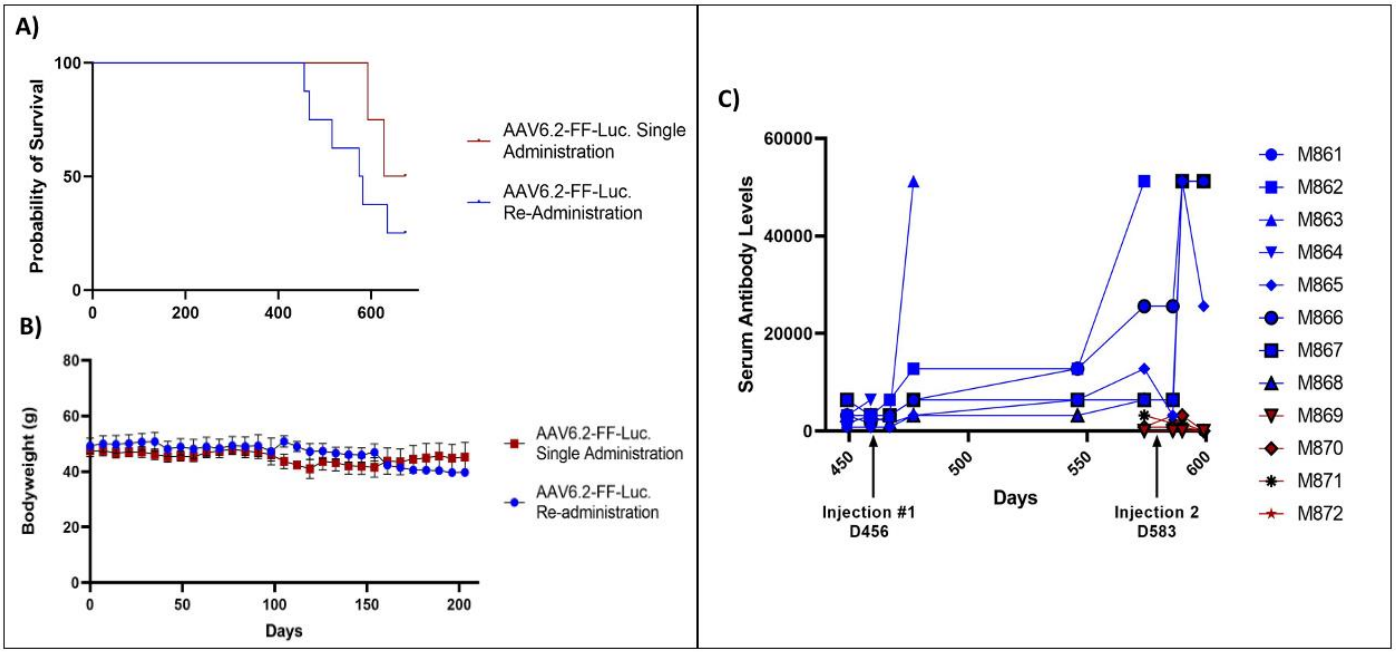

Figure 11. Antibody response to multiple re-administration of the AAV6.2-FF vector in SP-B mice. Kaplan-Meier survival curve **(A)** in mice beginning of D1 of life through to end of life. Bodyweight (g) measured from re-administration **(B). (C)** Periodic collection of serum antibodies to the AAV6.2-FF vector. Serum collected on D-3, D-1, D3, D7 following. administration.

5. DISCUSSION AND FUTURE DIRECTIONS

5.1 Discussion

5.1.1 The AAV6.2-FF approach in a model of Sftpc-L184Q pulmonary fibrosis

In this body of work we have shown the following: (1) The phenotype of the L184Q model of Sftpc-related pulmonary fibrosis aligns with the previously established model of I73T-*Sftpc* PF. (2) Investigations into previously observed inflammation and reported oxidative stress in the L184Q model did not demonstrate any significant pattern at baseline. (3) Subsequent administration with the AAV6.2-FF vector did not yield observable inflammation in L184Q mice. Nintedanib did not demonstrate significant impacts in the reduction of inflammation. (4) Re-administration of the AAV6.2-FF vector in adult mice who received *in-utero* administration does not significantly impact survival, bodyweight as a proxy for general health, and initial investigations show re-administration produces a typical antibody response.

Currently, pulmonary fibrosis is the most common reason for lung transplantation and while anti-fibrotic drugs are shown to slow progression, mortality is still estimated to occur between 3-5 years following diagnosis[38]. There are currently no therapies available for pulmonary fibrosis which aim to treat the genetic etiologies of the condition. Our lab has previously demonstrated the potential of a novel AAV platform for gene therapy, using the AAV6.2-FF vector developed by the Wootton Lab at the University of Guelph[29]. Our studies demonstrated a significant improvement in lifespan in a model of SP-B deficiency. This approach has also been used in a mouse model of bleomycin fibrosis associated with the *Sftpc*-I73T mutation and has demonstrated therapeutic potential (manuscript submitted). In the following studies, we aimed to assess the transfer of this successful therapy involving AAV6.2-FF to another *Sftpc* mutation (L184Q) in the previously established model of bleomycin fibrosis.

To do this, we characterized the LQ phenotype at baseline and in the model of bleomycin fibrosis. Bleomycin (@1U/kg) was administered, resulting in fibrotic injury of the lung. Bleomycin-treated mice demonstrated higher lung weight, worsened lung function, and significantly impacted lung structure quantified by histological scoring. These observations were made at the peak of the murine fibrosis cycle, on D17 following bleomycin administration. In this model, expected values of gene expression and protein expression were maintained with bleomycin administration, confirming the LQ phenotype.

The feasibility and safety of an AAV gene therapy is in part dependent on the immune response to the vector, as this may mediate the efficacy of the therapy. Assessing immune parameters is thus a critical component to the development of a successful AAV vector therapy. Increase in apoptosis and oxidative stress (OS) and inflammatory pathway activation in L184Q mice have previously been reported[21]. Additionally, preliminary experiments with the administration of AAV6.2-FF showed immune cell infiltration and inflammation in our lab, indicating a potentially inflammatory response to the AAV6.2-FF vector. To investigate this further, we assessed various markers of apoptosis and inflammation in L184Q mice. *Bax*, a marker of apoptosis, was previously shown to be up-regulated in L184Q mice at early postnatal timepoints. In our model, we found that *Bax* expression was significantly lower in LQ mice in vehicle and no treatment groups when compared to both WT and LQ-bleomycin groups[21]. This finding demonstrates the harmful effects of bleomycin on LQ lungs, with a marked increase in gene and protein expression of this pro-apoptotic marker. *Bax* is also a reported regulator of bleomycin fibrosis, and low levels of *Bax* have shown to increase fibroblast proliferation in pulmonary fibrosis[66]. A down-regulation of *Bax* in LQ mice may indicate regulation of fibroblast proliferation and apoptotic effects in LQ lungs.

A common inflammatory and oxidative stress marker in pulmonary fibrosis and pulmonary disease, *Nfe2l2*, was shown to be significantly decreased in LQ mice regardless of treatment group at both the protein and the gene expression levels. The *Nfe2l2* transcription factor is crucial in regulating the antioxidant response in the lungs and it's is linked with both Chronic Obstructive Pulmonary Disorder (COPD) and lung cancer[59]. As a result of this role in regulating the antioxidant response in the lungs, *Nfe2l2* is also thought to contribute to the development of Pulmonary Fibrosis, as ROS play a role in pathogenesis. In a knock-out model of radiation-induced pulmonary fibrosis, low levels of *Nfe2l2* were linked with lower amounts of alveoli and worse survival compared to wildtype mice[60]. Low levels of *Nfe2l2* in the L184Q model of disease may therefore indicate an aberrant anti-oxidant response and alterations in the ability of the L184Q mice to regulate a redox response in the lungs. Previous reports of decreased alveoli present in *Nfe2l2*-/- mice may also contribute to the observation of emphysema-like phenotype in the current L184Q model.

While the model of bleomycin-induced injury in *Sftpc*-L184Q closely recapitulated the I73T model of fibrosis, some differences were observed. Lung function values with the administration of bleomycin did not demonstrate any significant differences. AAV administration did not yield consistent MLI values. Altogether, it is our thinking that these factors in addition to histological appearance may indicate the L184Q mutation is associated with a more emphysema-like phenotype than the I73T mice. Significantly lower levels of *Nfe2l2* at both the protein and gene expression levels in these mice may provide more evidence, as *Nfe2l2*-/- mice were found to have distended and decreased amounts of alveoli compared to WT mice[60]. Further investigation into this unique phenotypic feature is warranted in order to understand how the present gene therapy approach can be best utilized in our model.

In addition to *Bax* and *Nfe2l2*, we also investigated levels of both *Nox2* and *Nox4* in our model, as these are known markers of oxidative stress in pulmonary fibrosis[61,63]. The Nox2 marker demonstrated a significant increase in gene and protein levels in bleomycin-treated mice, indicating active bleomycin fibrosis in the L184Q model of disease. However, no other differences in WT and LQ mice were observed. Significantly lower levels of *Nox4* gene expression was observed in all LQ animals regardless of treatment. In patients with IPF, *NOX4* has been shown to be increased[61]. The low levels of *Nox4* were not reflected in the levels of *Nox4* protein, and thus *Nox4* was not deemed a suitable marker in the L184Q model.

Together, these findings showed a significant change in a pro-apoptotic marker (*Bax*) and decreased levels of an important antioxidant regulator (*Nfe2l2*) in the model of L184Q bleomycin fibrosis, indicating a potential oxidative stress phenotype.

Clinically, anti-fibrotic drugs are prescribed for pulmonary fibrosis. Nintedanib is an anti-fibrotic prescribed for pulmonary fibrosis with both anti-fibrotic and anti-inflammatory properties. Given the markers indicating potential inflammation or oxidative stress in LQ mice, we then piloted Nintedanib in our model to assess the anti-inflammatory potential of this commonly prescribed drug. Ultimately, the combination of both the AAV gene therapy and Nintedanib may be a reasonable and translatable approach to treating *SFTPC*-related pulmonary fibrosis. In this pilot experiment, however, we were unable to detect consistent levels of the previously identified markers in our model. The administration of AAV6.2-FF did not appear to induce inflammation or oxidative stress as quantified by our markers. No changes in lung function or structure were detected. Nintedanib at the given concentration did not yield any changes in our model. These findings contribute to our confidence in applying the AAV6.2-FF based gene therapy to this model of L184Q bleomycin-fibrosis, as so significant adverse reaction

was demonstrated. Further investigations, for example a dose-response study, for Nintedanib may be useful in assessing the potential for a combination therapy of Nintedanib and AAV6.2-FF, a clinically relevant strategy for gene therapy.

Recently, our lab published work identifying the strong therapeutic potential of the AAV6.2-FF vector system for delivery to the lungs of SP-B deficient mice[29]. Given the promise of this therapeutic strategy, we aim to transfer this therapeutic to other surfactant protein disorders, including *Sftpc*-related PF. The L184Q model of pulmonary fibrosis demonstrates the potential for successful treatment with this system, as a successful recapitulation of the bleomycin fibrosis model and expression of an *Sftpc* transgene delivery by the AAV6.2-FF vector *in vivo* was shown.

5.1.2 Assessing feasibility of Re-administration in adult mice given gene therapy In-utero

Clinically, SP-B deficiency presents shortly after birth as respiratory distress and respiratory failure leading to neonatal death[29]. Previously published work by Kang et al, 2020 published by our laboratory has demonstrated significant success in extending the lifespan of SP-B deficient mice, as discussed[29]. While this inducible model of SP-B deficiency captures much of the clinical situation, it is unable to capture the clinical course of the condition from birth. Attempting to capture the clinical timeline more closely in this model, members of our lab began piloting *in-utero* administration of the AAV gene therapy to assess the feasibility of treatment in a true, non-inducible model of SP-B knock-out at birth. Models of *in-utero* treatment have been explored in conditions related to the pulmonary epithelium, as demonstrated by Sekhon et al, who successful administered Adenovirus gene therapy *in-utero*[62]. Here we aimed to assess major health concerns with this approach by monitoring longterm survival and health of these mice over time. No significant impacts on survival and bodyweight in mice administered AAV6.2-FF-

Luc gene therapy prenatally were observed. Administration and transduction was confirmed by *in vivo* imaging.

A primary challenge in viral vector-based gene therapy is the immune response to the vector capsid[64]. Immunity through previously mounted antibodies to the viral serotype can cause adverse reactions to the therapy and reduce efficacy of treatment and is a major consideration for the transfer of potential AAV-based therapeutics to the clinic[64].

Given the unique cohort of mice treated prenatally, we aimed to assess the presence of antibodies to the viral vector from given further administrations in adulthood. The antibody reaction in re-administrated adults did not stray from expected outcomes, demonstrating antibodies upon first administration and an increase in antibody response upon second administration. While further investigations are required, this indicates that the antibody response to the AAV6.2-FF vector may not be altered with *in-utero* injection. These findings also provide us with insight into the idea of innate immunity to the AAV6.2-FF antibody. Given prenatal exposure prior to the maturation of the immune system, it was considered that an innate tolerance to the viral vector could be possible, and that subsequent administration may not lead to a reaction. However, adult administration revealed an expected response.

5.2 Future Directions

The transferability of the AAV6.2-FF system to multiple conditions or genetic etiologies is an important aspect of the therapeutic, as it provides the potential for treatment of multiple conditions using the same therapeutic. Characterization and understanding of the unique nature of each model of disease is therefore crucial to the development of this gene therapy system and the clinical significance. Further areas of exploration in the LQ model might address the suspected emphysema-like characteristics of these mice, in order to properly assess therapeutic

potential of the AAV gene therapy. With both a preliminary response to the vector and phenotyping of the L184Q model presented, further understanding into the treatment of fibrosis in the L184Q bleomycin model would cement the transferability of the therapeutic from the I73T model to the L184Q model. With this, multiple etiologies of pulmonary fibrosis could be treated with the same genetic therapy. Additionally, a dose-response study of Nintedanib in the LQ model and explorations of this drug in combination with the AAV6.2-FF-*Sftpc* system could provide a clinically relevant and realistic approach to treat pulmonary fibrosis in humans as this is one of the most commonly prescribed drugs for pulmonary fibrosis. Assessing interactions between the drug and the AAV6.2-FF system could also provide insight into the safety of this treatment for patients who are not treatment-naïve.

In the model of prenatal administration of the the AAV6.2-FF system, follow up experiments might include administering *in-utero* gene therapy to mice in an induced model of expression, where knock-out is induced early in life. Additionally exploring prenatal therapy in a complete knock-out might be feasible. Furthermore, exploration of the AAV6.2-FF immune and antibody response in the SP-B model of re-administration is ongoing in our lab (manuscript submitted). Immune-modulatory strategies have been employed to suppress the response to the AAV6.2-FF vector re-administered in adulthood by mTOR signalling. The aim of this is prolonging *Sftpb* expression and further extending the lifespan of SP-B deficient mice. As these investigations have shown promise, the application of immune-modulatory strategies might be applicable to mice treated prenatally, as this may help mediate adult re-administration.

6. CONCLUSION

In conclusion, this thesis explores the transferability of the promising AAV6.2-FF gene therapy system to two different models of surfactant protein deficiencies by exploring unique characteristics of the models. It also explores the development of a model of bleomycin fibrosis in an additional mutation of *SFTPC*-related pulmonary fibrosis. This was done using baseline assessment of lung function, lung structure, and expression. We showed the applicability of the AAV6.2-FF treatment to these models and piloted a potential combinatorial strategy. Further exploration of the AAV6.2-FF-*Sftpc* therapeutic is required.

7. REFERENCES

1. Davies, A., & Moores, C. (2010). Structure of the Respiratory System, Related to Function. *The Respiratory System,* 11–28. https://doi.org/10.1016/B978-0-7020-3370-4.00002-5
2. Knudsen, L., & Ochs, M. (2018). The micromechanics of lung alveoli: structure and function of surfactant and tissue components. Histochemistry and cell biology, 150(6), 661–676. https://doi.org/10.1007/s00418-018-1747-9
3. Creuwels, L. A., van Golde, L. M., & Haagsman, H. P. (1997). The pulmonary surfactant system: biochemical and clinical aspects. Lung, 175(1), 1–39. https://doi.org/10.1007/pl00007554
4. Bernhard W. (2016). Lung surfactant: Function and composition in the context of development and respiratory physiology. Annals of anatomy = Anatomischer Anzeiger : official organ of the Anatomische Gesellschaft, 208, 146–150. https://doi.org/10.1016/j.aanat.2016.08.003
5. Whitsett, J. A., Wert, S. E., & Weaver, T. E. (2010). Alveolar surfactant homeostasis and the pathogenesis of pulmonary disease. *Annual review of medicine, 61*, 105–119. https://doi.org/10.1146/annurev.med.60.041807.123500
6. Possmayer, F., Nag, K., Rodriguez, K., Qanbar, R., & Schürch, S. (2001). Surface activity in vitro: role of surfactant proteins. *Comparative biochemistry and physiology. Part A, Molecular & integrative physiology, 129*(1), 209–220. https://doi.org/10.1016/s1095-6433(01)00317-8

7. Abdel-Razek, O., Liu, T., Chen, X., Wang, Q., Vanga, G., & Wang, G. (2021). Role of Surfactant Protein D in Experimental Otitis Media. *Journal of innate immunity*, *13*(4), 197–210. https://doi.org/10.1159/000513605
8. Han, S., & Mallampalli, R. K. (2015). The Role of Surfactant in Lung Disease and Host Defense against Pulmonary Infections. *Annals of the American Thoracic Society*, *12*(5), 765–774. https://doi.org/10.1513/AnnalsATS.201411-507FR
9. Hillaire, M. L., Haagsman, H. P., Osterhaus, A. D., Rimmelzwaan, G. F., & van Eijk, M. (2013). Pulmonary surfactant protein D in first-line innate defence against influenza A virus infections. *Journal of innate immunity*, *5*(3), 197–208. https://doi.org/10.1159/000346374
10. King, B. A., & Kingma, P. S. (2011). Surfactant protein D deficiency increases lung injury during endotoxemia. *American* journal of respiratory cell and molecular biology, 44(5), 709–715. https://doi.org/10.1165/rcmb.2009-0436OC
11. Whitsett, J. A., & Weaver, T. E. (2002). Hydrophobic surfactant proteins in lung function and disease. *New England Journal of Medicine*, *347*(26), 2141–2148. https://doi.org/10.1056/nejmra022387
12. Nogee L. M. (2019). Genetic causes of surfactant protein abnormalities. *Current opinion in pediatrics*, *31*(3), 330–339. https://doi.org/10.1097/MOP.0000000000000751
13. Whitsett, J. A., Nogee, L. M., Weaver, T. E., & Horowitz, A. D. (1995). Human surfactant protein B: structure, function, regulation, and genetic disease. Physiological reviews, 75(4), 749–757. https://doi.org/10.1152/physrev.1995.75.4.749
14. Beers, M. F., & Fisher, A. B. (1992). Surfactant protein C: a review of its unique properties and metabolism. *The American journal of physiology*, *263*(2 Pt 1), L151–L160. https://doi.org/10.1152/ajplung.1992.263.2.L151

15. Dickens, J. A., Rutherford, E. N., Abreu, S., Chambers, J. E., Ellis, M. O., van Schadewijk, A., Hiemstra, P. S., & Marciniak, S. J. (2021). Novel insights into surfactant protein C trafficking revealed through the study of a pathogenic mutant. *European Respiratory Journal, 59*(1), 2100267. https://doi.org/10.1183/13993003.00267-2021

16. Thompson, M. W. (2001). Surfactant Protein B Deficiency: Insights into Surfactant Function through Clinical Surfactant Protein Deficiency. *The American Journal of the Medical Sciences, 321*(1), 26–32. https://doi.org/10.1097/00000441-200101000-00005

17. Wilder M. A. (2004). Surfactant protein B deficiency in infants with respiratory failure. *The Journal of perinatal & neonatal nursing, 18*(1), 61–67. https://doi.org/10.1097/00005237-200401000-00006

18. Autilio, C., & Pérez-Gil, J. (2019). Understanding the principle biophysics concepts of pulmonary surfactant in health and disease. Archives of disease in childhood. *Fetal and neonatal edition, 104*(4), F443–F451. https://doi.org/10.1136/archdischild-2018-315413

19. Nogee, L. M., & Trapnell, B. C. (2019). Lung diseases associated with disruption of pulmonary surfactant homeostasis. *Kendig's Disorders of the Respiratory Tract in Children*. https://doi.org/10.1016/b978-0-323-44887-1.00057-2

20. Ikegami, M., & Jobe, A. H. (1998). Surfactant protein metabolism in vivo. *Biochimica et biophysica acta, 1408*(2-3), 218–225. https://doi.org/10.1016/s0925-4439(98)00069-6

21. Sitaraman, S., Martin, E. P., Na, C. L., Zhao, S., Green, J., Deshmukh, H., Perl, A. T., Bridges, J. P., Xu, Y., & Weaver, T. E. (2021). Surfactant protein C mutation links postnatal type 2 cell dysfunction to adult disease. *JCI insight, 6*(14), e142501. https://doi.org/10.1172/jci.insight.142501

22. Young WA. Familial fibrocystic pulmonary dysplasia: a new case in a known affected family. *Can Med Assoc* J. *1966*;*94*(20):1059–1061.

23. Katzen, J., Wagner, B. D., Venosa, A., Kopp, M., Tomer, Y., Russo, S. J., Headen, A. C., Basil, M. C., Stark, J. M., Mulugeta, S., Deterding, R. R., & Beers, M. F. (2019). An SFTPC BRICHOS mutant links epithelial ER stress and spontaneous lung fibrosis. *JCI insight*, *4*(6), e126125. https://doi.org/10.1172/jci.insight.126125

24. Maguire, J. A., Mulugeta, S., & Beers, M. F. (2011). Endoplasmic reticulum stress induced by surfactant protein C Brichos Mutants promotes proinflammatory signaling by epithelial cells. *American Journal of Respiratory Cell and Molecular Biology*, *44*(3), 404–414. https://doi.org/10.1165/rcmb.2009-0382oc

25. van Riet, S., van Schadewijk, A., Khedoe, P. P. S. J., Limpens, R. W. A. L., Bárcena, M., Stolk, J., Hiemstra, P. S., & van der Does, A. M. (2022). Organoid-based expansion of patient-derived primary alveolar type 2 cells for establishment of alveolus epithelial Lung-Chip cultures. *American journal of physiology. Lung cellular and molecular physiology*, *322*(4), L526–L538. https://doi.org/10.1152/ajplung.00153.2021

26. Glisinski, K. M., Schlobohm, A. J., Paramore, S. V., Birukova, A., Moseley, M. A., Foster, M. W., & Barkauskas, C. E. (2020). Interleukin-13 disrupts type 2 pneumocyte stem cell activity. *JCI insight*, *5*(1), e131232. https://doi.org/10.1172/jci.insight.131232

27. Munis, A. M., Hyde, S. C., & Gill, D. R. (2021). A human surfactant B deficiency air-liquid interface cell culture model suitable for gene therapy applications. *Molecular Therapy - Methods & Clinical Development*, *20*, 237–246. https://doi.org/10.1016/j.omtm.2020.11.013

28. van Riet, S., Ninaber, D.K., Mikkers, H.M.M. et al. (2020). In vitro modelling of alveolar repair at the air-liquid interface using alveolar epithelial cells derived from human induced pluripotent stem cells. *Sci Rep 10*, 5499. https://doi.org/10.1038/s41598-020-62226-1

29. Kang, M. H., van Lieshout, L. P., Xu, L., Domm, J. M., Vadivel, A., Renesme, L., Mühlfeld, C., Hurskainen, M., Mižíková, I., Pei, Y., van Vloten, J. P., Thomas, S. P., Milazzo, C., Cyr-Depauw, C., Whitsett, J. A., Nogee, L. M., Wootton, S. K., & Thébaud, B. (2020). A lung tropic AAV vector improves survival in a mouse model of surfactant B deficiency. *Nature communications*, *11*(1), 3929. https://doi.org/10.1038/s41467-020-17577-8

30. Wilder M. A. (2004). Surfactant protein B deficiency in infants with respiratory failure. *The Journal of perinatal & neonatal nursing*, *18*(1), 61–67. https://doi.org/10.1097/00005237-200401000-00006

31. Nureki, S.-I., Tomer, Y., Venosa, A., Katzen, J., Russo, S. J., Jamil, S., Barrett, M., Nguyen, V., Kopp, M., Mulugeta, S., & Beers, M. F. (2018). Expression of mutant sftpc in murine alveolar epithelia drives spontaneous lung fibrosis. *Journal of Clinical Investigation*, *128*(9), 4008–4024. https://doi.org/10.1172/jci99287

32. Chanda, D., Otoupalova, E., Smith, S. R., Volckaert, T., De Langhe, S. P., & Thannickal, V. J. (2019). Developmental pathways in the pathogenesis of lung fibrosis. *Molecular aspects of medicine*, *65*, 56–69. https://doi.org/10.1016/j.mam.2018.08.004

33. Demedts, M., Wells, A. U., Anto, J. M., Costabel, U., Hubbard, R., Cullinan, P., ... & Taylor, A. N. (2001). Interstitial lung diseases: an epidemiological overview. *European respiratory journal*, *18*(32 suppl), 2S-16S.

34. Wijsenbeek, M., Suzuki, A., & Maher, T. M. (2022). Interstitial lung diseases. *The Lancet*, *400*(10354), 769-786.

35. Günther, A., Korfei, M., Mahavadi, P., von der Beck, D., Ruppert, C., & Markart, P. (2012). Unravelling the progressive pathophysiology of idiopathic pulmonary fibrosis. *European Respiratory Review*, *21*(124), 152-160.

36. Loomis-King, H., Flaherty, K. R., & Moore, B. B. (2013). Pathogenesis, current treatments and future directions for idiopathic pulmonary fibrosis. *Current opinion in pharmacology*, *13*(3), 377–385. https://doi.org/10.1016/j.coph.2013.03.015

37. Somogyi, V., Chaudhuri, N., Torrisi, S. E., Kahn, N., Müller, V., & Kreuter, M. (2019). The therapy of idiopathic pulmonary fibrosis: what is next?. *European respiratory review : an official journal of the European Respiratory Society*, *28*(153), 190021. https://doi.org/10.1183/16000617.0021-2019

38. Glass, D. S., Grossfeld, D., Renna, H. A., Agarwala, P., Spiegler, P., DeLeon, J., & Reiss, A. B. (2022). Idiopathic pulmonary fibrosis: Current and future treatment. *The clinical respiratory journal*, *16*(2), 84–96. https://doi.org/10.1111/crj.13466

39. Nerelius, C., Martin, E., Peng, S., Gustafsson, M., Nordling, K., Weaver, T., & Johansson, J. (2008). Mutations linked to interstitial lung disease can abrogate anti-amyloid function of prosurfactant protein C. The Biochemical journal, 416(2), 201–209. https://doi.org/10.1042/BJ20080981

40. Lawson, W. E., Grant, S. W., Ambrosini, V., Womble, K. E., Dawson, E. P., Lane, K. B., ... & Du Bois, R. M. (2004). Genetic mutations in surfactant protein C are a rare cause of sporadic cases of IPF. *Thorax*, *59*(11), 977-980.

41. Nogee, L. M., Dunbar, A. E., Wert, S. E., Askin, F., Hamvas, A., & Whitsett, J. A. (2001). A mutation in the surfactant protein C gene associated with familial interstitial lung

disease. *New England Journal of Medicine*, *344*(8), 573–579. https://doi.org/10.1056/nejm200102223440805

42. Santangelo, S., Scarlata, S., Zito, A., Chiurco, D., Pedone, C., & Incalzi, R. A. (2013). Genetic background of idiopathic pulmonary fibrosis. *Expert Review of Molecular Diagnostics*, *13*(4), 389–406. https://doi.org/10.1586/erm.13.22
43. Mouratis, M. A., & Aidinis, V. (2011). Modeling pulmonary fibrosis with Bleomycin. *Current Opinion in Pulmonary Medicine*, *17*(5), 355–361. https://doi.org/10.1097/mcp.0b013e328349ac2b
44. Liu, T., De Los Santos, F. G., & Phan, S. H. (2017). The Bleomycin Model of Pulmonary Fibrosis. *Methods in molecular biology*, 1627, 27–42. https://doi.org/10.1007/978-1-4939-7113-8_2
45. Kolb, P., Upagupta, C., Vierhout, M., Ayaub, E., Bellaye, P. S., Gauldie, J., Shimbori, C., Inman, M., Ask, K., & Kolb, M. R. J. (2020). The importance of interventional timing in the bleomycin model of pulmonary fibrosis. The European respiratory journal, 55(6), 1901105. https://doi.org/10.1183/13993003.01105-2019
46. Walters, D. M., & Kleeberger, S. R. (2008). Mouse models of bleomycin-induced pulmonary fibrosis. *Current Protocols in Pharmacology*, *40*(1). https://doi.org/10.1002/0471141755.ph0546s40
47. Laporta Hernandez, R., Aguilar Perez, M., Lázaro Carrasco, M. T., & Ussetti Gil, P. (2018). Lung Transplantation in Idiopathic Pulmonary Fibrosis. *Medical sciences (Basel, Switzerland)*, *6*(3), 68. https://doi.org/10.3390/medsci6030068
48. Wollin, L., Maillet, I., Quesniaux, V., Holweg, A., & Ryffel, B. (2014). Antifibrotic and anti-inflammatory activity of the tyrosine kinase inhibitor nintedanib in experimental models of

lung fibrosis. *The Journal of pharmacology and experimental therapeutics, 349*(2), 209–220. https://doi.org/10.1124/jpet.113.208223

49. Pan, L., Cheng, Y., Yang, W., Wu, X., Zhu, H., Hu, M., Zhang, Y., & Zhang, M. (2023). Nintedanib Ameliorates Bleomycin-Induced Pulmonary Fibrosis, Inflammation, Apoptosis, and Oxidative Stress by Modulating PI3K/Akt/mTOR Pathway in Mice. *Inflammation, 46*(4), 1531–1542. https://doi.org/10.1007/s10753-023-01825-2
50. Trachalaki, A., Sultana, N., & Wells, A. U. (2023). An update on current and emerging drug treatments for idiopathic pulmonary fibrosis. *Expert Opinion on Pharmacotherapy, 24*(10), 1125–1142. https://doi.org/10.1080/14656566.2023.2213436
51. Conte, E., Gili, E., Fagone, E., Fruciano, M., Iemmolo, M., & Vancheri, C. (2014). Effect of pirfenidone on proliferation, TGF-β-induced myofibroblast differentiation and fibrogenic activity of primary human lung fibroblasts. *European Journal of Pharmaceutical Sciences, 58*(Complete), 13–19. https://doi.org/10.1016/j.ejps.2014.02.014
52. Ley, B., Swigris, J., Day, B. M., Stauffer, J. L., Raimundo, K., Chou, W., & Collard, H. R. (2017). Pirfenidone Reduces Respiratory-related Hospitalizations in Idiopathic Pulmonary Fibrosis. *American journal of respiratory and critical care medicine, 196*(6), 756–761. https://doi-org.myaccess.library.utoronto.ca/10.1164/rccm.201701-0091OC
53. Richeldi, L., Cottin, V., du Bois, R. M., Selman, M., Kimura, T., Bailes, Z., Schlenker-Herceg, R., Stowasser, S., & Brown, K. K. (2016). Nintedanib in patients with idiopathic pulmonary fibrosis: Combined evidence from the TOMORROW and INPULSIS® trials. *Respiratory Medicine, 113*(Complete), 74–79. https://doi.org/10.1016/j.rmed.2016.02.001

54. Cooney, A. L., Wambach, J. A., Sinn, P. L., & McCray, P. B., Jr (2022). Gene Therapy Potential for Genetic Disorders of Surfactant Dysfunction. *Frontiers in genome editing, 3,* 785829. https://doi.org/10.3389/fgeed.2021.785829

55. Percie du Sert N, et al.(2020). The ARRIVE guidelines 2.0: Updated guidelines for reporting animal research. *PLoS Biol.* doi*:* 10.1371/journal.pbio.3000410.

56. AVERY, M. E. (1959). Surface properties in relation to atelectasis and hyaline membrane disease. *Archives of Pediatrics & Adolescent Medicine*, *97*(5_PART_I), 517. https://doi.org/10.1001/archpedi.1959.02070010519001

57. Edwards, L. A., Read, L. C., Nishio, S. J., Weir, A. J., Hull, W., Barry, S., Styne, D., Whitsett, J. A., Tarantal, A. F., & George-Nascimento, C. (1995). Comparison of the distinct effects of epidermal growth factor and betamethasone on the morphogenesis of the gas exchange region and differentiation of alveolar type II cells in lungs of fetal rhesus monkeys. *The Journal of Pharmacology and Experimental Therapeutics, 274*(2), 1025–1032.

58. Limjunyawong, N., Fallica, J., Horton, M. R., & Mitzner, W. (2015). Measurement of the pressure-volume curve in mouse lungs. *Journal of Visualized Experiments*, (95). https://doi.org/10.3791/52376

59. Sandford, A. J., Malhotra, D., Boezen, H. M., Siedlinski, M., Postma, D. S., Wong, V., Akhabir, L., He, J.-Q., Connett, J. E., Anthonisen, N. R., Paré, P. D., & Biswal, S. (2012b). *nfe2l2* pathway polymorphisms and lung function decline in chronic obstructive pulmonary disease. *Physiological Genomics*, *44*(15), 754–763. https://doi.org/10.1152/physiolgenomics.00027.2012

60. Travis, E. L., Rachakonda, G., Zhou, X., Korhonen, K., Sekhar, K. R., Biswas, S., & Freeman, M. L. (2011). NRF2 deficiency reduces life span of mice administered thoracic

irradiation. *Free Radical Biology and Medicine*, *51*(6), 1175–1183. https://doi.org/10.1016/j.freeradbiomed.2011.05.038

61. Hecker, L., Cheng, J., & Thannickal, V. J. (2012). Targeting NOX enzymes in pulmonary fibrosis. *Cellular and molecular life sciences : CMLS*, *69*(14), 2365–2371. https://doi.org/10.1007/s00018-012-1012-7
62. Sekhon, H., Larson, J. In utero gene transfer into the pulmonary epithelium. (1995). *Nat Med 1*, 1201–1203. https://doi.org/10.1038/nm1195-1201
63. Lee, S. H., Shin, M. H., Leem, A. Y., Lee, S. H., Chung, K. S., Kim, Y. S., & Park, M. S. (2022). NADPH oxidase 4 signaling in a ventilator-induced lung injury mouse model. *Respiratory research*, *23*(1), 73. https://doi.org/10.1186/s12931-022-01992-0
64. Kohn, D. B., Chen, Y. Y., & Spencer, M. J. (2023). Successes and challenges in clinical gene therapy. Gene therapy, 30(10-11), 738–746. https://doi.org/10.1038/s41434-023-00390-5
65. Chen, M., Kim, B., Jarvis, M. I., Fleury, S., Deng, S., Nouraein, S., Butler, S., Lee, S., Chambers, C., Hodges, H. C., Szablowski, J. O., Suh, J., & Veiseh, O. (2023). Immune profiling of adeno-associated virus response identifies B cell-specific targets that enable vector re-administration in mice. *Gene therapy*, *30*(5), 429–442. https://doi.org/10.1038/s41434-022-00371-0
66. Suzuki, K., Yanagihara, T., Yokoyama, T., Maeyama, T., Ogata-Suetsugu, S., Arimura-Omori, M., Mikumo, H., Hamada, N., Harada, E., Kuwano, K., Harada, T., & Nakanishi, Y. (2017). Bax-inhibiting peptide attenuates bleomycin-induced lung injury in mice. *Biology open*, *6*(12), 1869–1875. https://doi.org/10.1242/bio.026005

7. APPENDIX

Representative Western Blot Images

proSP-C

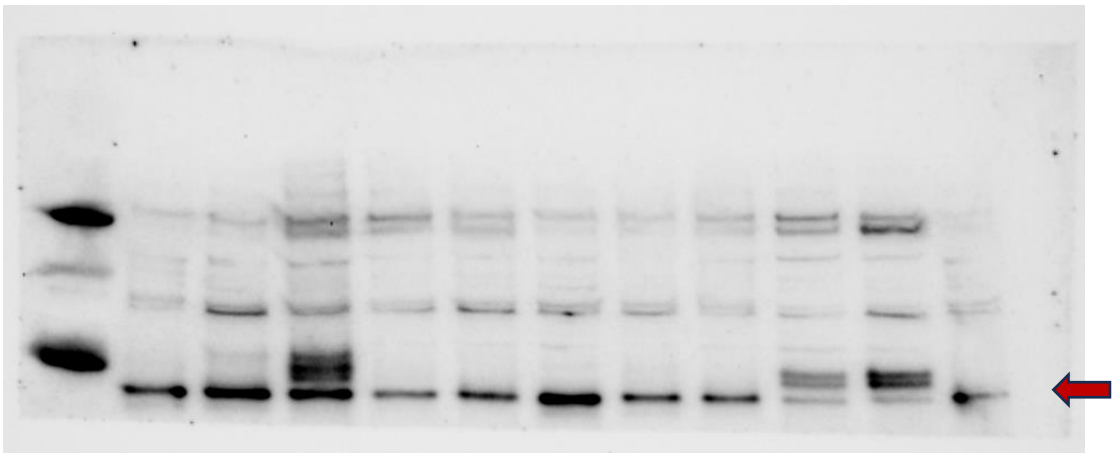

matureSP-C